

RESEARCH ARTICLE

Toward the proteome of the human peripheral blood eosinophil

Christof Straub¹, Konrad Pazdrak¹, Travis W. Young^{1*}, Susan J. Stafford², Zheng Wu^{1,2}, John E. Wiktorowicz^{1,2,3}, Anthony M. Haag², Robert D. English², Kizhake V. Soman^{1,2,3} and Alexander Kurosky^{1,2,3}

¹ Department of Biochemistry and Molecular Biology, University of Texas Medical Branch, Galveston, TX, USA

² The UTMB Biomolecular Resource Facility, University of Texas Medical Branch, Galveston, TX, USA

³ The UTMB NHLBI Proteomics Center, University of Texas Medical Branch, Galveston, TX, USA

Eosinophils (EOSs) are granular leukocytes that have significant roles in many inflammatory and immunoregulatory responses, especially asthma and allergic diseases. We have undertaken a fairly comprehensive proteomic analysis of purified peripheral blood EOSs from normal human donors primarily employing 2-DE with protein spot identification by MALDI-MS. Protein subfractionation methods employed included IEF (Zoom[®] Fractionator) and subcellular fractionation using differential protein solubilization. We have identified 3141 proteins, which had Mascot expectation scores of 10^{-3} or less. Of these 426 were unique and non-redundant of which 231 were novel proteins not previously reported to occur in EOSs. Ingenuity Pathway Analysis showed that some 70% of the non-redundant proteins could be subdivided into categories that are clearly related to currently known EOS biological activities. Cytoskeletal and associated proteins predominated among the proteins identified. Extensive protein posttranslational modifications were evident, many of which have not been previously reported that reflected the dynamic character of the EOS. This data set of eosinophilic proteins will prove valuable in comparative studies of disease *versus* normal states and for studies of gender differences and polymorphic variation among individuals.

Received: March 14, 2009

Revised: May 5, 2009

Accepted: June 10, 2009

**Keywords:**

2-DE / Asthma / Eosinophils / Phosphoproteins / Protein expression

1 Introduction

Eosinophils (EOS) are pleiotropic multifunctional granulocytic leukocytes that function in diverse inflammatory and immunoregulatory responses (see reviews [1, 2]). Important pathologies associated with EOSs include asthma, allergy,

and parasitic helminth infections [1, 3]. In normal adults, EOSs are produced, differentiated, and matured in the bone marrow, migrate into the peripheral blood, and subsequently target to different tissues including mammary gland, thymus, uterus, lung, and especially the gastrointestinal tract [1]. However, in many inflammatory pathologies EOSs can also be associated with numerous other organs and tissues. EOS trafficking into inflammatory sites involves a number of cytokines, chemokines, growth factors, lipids, as well as four major cationic proteins (EOS peroxidase (EPO), major basic proteins (MBP), EOS cationic protein (ECP), EOS-derived neurotoxin (EDN)) packaged within four types of cytoplasmic granules each with unique morphologies [1, 4].

Correspondence: Dr. Alexander Kurosky, Department of Biochemistry and Molecular Biology, The University of Texas Medical Branch, 301 University Boulevard, Galveston, TX 77555-0635, USA

E-mail: akurosky@utmb.edu

Fax: +1-409-772-8025

Abbreviations: ECP, eosinophil cationic protein; EDN, eosinophil-derived neurotoxin; EOS, eosinophil; EPO, eosinophil peroxidase; HBSS, Hank's balanced saline solution; ID, identification; IPA, Ingenuity Pathway Analysis; MBP, major basic protein; RT, room temperature

*Current address: Center for Technology Development, Texas A&M University, College Station, TX, USA.

Most current established methods of preparing EOSs from peripheral blood utilizing anti-CD16 immunomagnetic beads to remove neutrophils yield a population of cells which is relatively homogenous, typically greater than 98% [5]. However, density gradient centrifugation can further distinguish two populations of EOSs termed “normodense” (specific gravity >1.085 g/L) and “hypodense” (specific gravity <1.085 g/L) [6]. Hypodense EOSs typically account for 5–10% of the total peripheral blood EOS population in normal adults and represent activated and degranulated cells [7]. Normodense EOSs can be converted to a hypodense form *in vitro* by a number of different stimuli; *e.g.* granulocyte-macrophage colony-stimulating factor, interleukin-3, eotaxin, and interleukin-5 [8]. Moreover, in much inflammatory pathology the hypodense population of cells is increased; however, the composition of these hypodense EOSs can differ when compared with *in vitro* stimulated cells [4, 8, 9]. Therefore, within the hypodense population of EOSs there is indication of further microheterogeneity likely due to differential degranulation depending on the nature of the stimulus employed or the pathology involved. Thus, the molecular basis for all of the observed EOS heterogeneity is not fully established and clearly requires further investigation. A comparative proteome map of EOSs from normal adults would be considerably important toward defining EOS heterogeneity, especially in inflammatory diseases.

It is clear that EOSs play an important role in the etiology of bronchial asthma, which is one of the fastest growing diseases in the Western world. The prevalence of asthma has increased steadily over the last two decades and in 2006 an estimated 16.1 million adults (7.3% >18 years) and some 9.4% or 6.8 million children were affected by the disease in the United States [10]. The rapid increase in the incidence of asthma and its resulting consequence on the healthcare system underscores the need for the identification (ID) of new therapeutic targets for the treatment of allergic inflammation. None of the currently available treatments for asthma and allergic diseases are curative. Recently, a number of factors have been proposed which appear to control EOS trafficking, survival and activation in animal models; however, to date, no therapeutic target has been developed which successfully eliminates tissue-activated EOSs in human trials. Furthermore, the dual role of EOSs in pro-inflammation and anti-inflammation has yet to be elucidated fully. Together these findings clearly emphasize the current status of an incomplete understanding of EOS activation and function, and argue for more comprehensive studies of the EOS phenotype.

We hypothesize that an unbiased characterization of a comprehensive set of proteins expressed by EOSs will provide novel insights into the molecular circuitry, signaling pathways, pro-inflammatory mediators, and cytokines that may play a role in the pathogenesis of EOS inflammation. Furthermore, the map will be important in comparative EOS studies of disease or therapeutic treatments. In the present work, we initiated the proteomic characterization of

peripheral blood EOSs obtained from healthy, non-allergic donors. Furthermore, in order to decrease the complexity of the cell lysate and maximize the total number of proteins identified in the study, we fractionated the cell lysate into cytoplasmic, membrane, organelle, and nuclear fractions, and resolved the proteins by 2-DE. We report a number of proteins that are unique to EOSs and are associated with EOS effector functions. We posit that the present data will therefore serve as an important reference database for the discovery of markers of activated EOSs and for future studies investigating therapeutic targets for eosinophilia-related inflammatory diseases.

2 Materials and methods

2.1 Materials

Histopaque[®]-1077, CHCA, benzamidine, leupeptin, aprotinin, microcystin, and dextran (Fluka) were obtained from Sigma-Aldrich (St. Louis, MO, USA). Sodium orthovanadate and PMSF were products of Fisher Scientific (Fair Lawn, NJ, USA). Thiourea, CHAPS, iodoacetamide, IPG strips (pH 5–8), Precision Plus molecular weight standards, Protean II XL Tris-HCl precast gels (8–16%), Criterion Tris-HCl precast gels (8–16%), RC DC protein assay kit (Lowry method with reduction compatibility (RC) and detergent compatibility (DC), Criterion Dodeca electrophoretic 13.3 cm \times 8.7 cm multi-gel cell (12 gels, 11 cm strips) and Protean II XL electrophoretic 19.3 cm \times 18.3 cm cell (2 gels, 18 cm strips) were products from Bio-Rad (Hercules, CA, USA). IPG strips (11 and 18 cm, pH 3–10, 4–7, and 6–11), DeStreak rehydration buffer, IPG buffer/ampholytes, and Ettan DALT IPGphor II IEF cell were obtained from GE Healthcare. Tri-(2-carboxyethyl) phosphine and Perfect-FOCUS (protein precipitation reagent for 2-DE samples) were purchased from G-Biosciences (St. Louis, MO, USA). Sypro Ruby fluorescent protein gel stain, Pro-Q Diamond fluorescent phosphoprotein gel stain, Peppermint Stick phosphoprotein molecular weight markers, and a Zoom[®] IEF fractionator were obtained from Invitrogen (Carlsbad, CA, USA). Hank's balanced saline solution (HBSS) without Mg^{2+} or Ca^{2+} was from Gibco. The ProteoExtract[®] Subcellular Proteome Extraction kit was from Calbiochem (San Diego, CA, USA). VarioMACS separation columns, MACS Separator (magnetic), and CD16 MicroBeads for EOS isolation were purchased from Miltenyi Biotec (Auburn, CA, USA).

2.2 EOS isolation from peripheral human blood

Blood donors for EOS isolation included three female and five male non-smoking donors (ages 18–50 years) who showed neither asthmatic nor allergic symptoms [5]. Briefly, 1.5 mL of 15% dextran and 1.5 mL of 0.25 M EDTA were

immediately added to 60 mL of collected blood in two 50 mL polypropylene conical centrifuge tubes and allowed to sediment for 30 min at room temperature (RT). After sedimentation, the leukocyte-containing layer was overlaid onto Histopaque[®]-1077 (15 mL leukocyte/7.5 mL Histopaque[®]) and centrifuged ($720 \times g$) at RT for 40 min. Following washing at 4°C with 20 mM HEPES-1 \times HBSS, granulocytes were recovered by centrifugation ($300 \times g$ for 7 min) and any remaining erythrocytes were lysed with consecutive additions of 5 mL of ice-cold 0.2% NaCl for 30 s followed by 5 mL of 1.8% NaCl. Following the further addition of 20 mL of HBSS, cells were centrifuged at $300 \times g$ for 7 min at 4°C. EOSs were subsequently isolated by negative selection using CD16⁺ MicroBeads as instructed by the manufacturer (Miltenyi Biotec). Briefly, CD16⁺ cells (essentially neutrophils) were labeled with CD16⁺ MicroBeads and the cell suspension was loaded onto a VarioMACS column. The column was placed in the magnetic field of a MACS Separator and the labeled CD16⁺ cells were retained on the column. Unlabeled purified EOSs were not retained and were washed out and collected. After removal of the column from the magnetic field, the neutrophil fraction was eluted from the column. EOS purity was consistently monitored by Hansel staining and typically ranged above 98%. The levels of activated EOSs in our preparations ranged between 1–3% as estimated by measurement of the activation marker CD69 [11].

2.3 2-DE sample preparation

Following CD16⁺ MicroBead EOS isolation, cells were pelleted at $300 \times g$ and washed with 30 mL of 1 \times HBSS. After additional centrifugation at $300 \times g$ for 7 min cells were solubilized for 2-DE in DeStreak rehydration buffer to a protein concentration of 1 $\mu\text{g}/\mu\text{L}$. If not used immediately for IEF, samples were stored at -80°C . EOSs were also subjected to subcellular fractionation using Calbiochem's ProteoExtract[®] Subcellular Proteome Extraction kit according to the manufacturer's provided protocol. Some samples were also subjected to IEF fractionation using a ZOOM[®] IEF Fractionator (Invitrogen) following the manufacturer's provided protocol. Ranges of pH collected were 3.0–5.4, 5.4–7.0, and 7.0–10.0. Protein concentrations were established using the RC DC protein assay kit (Bio-Rad). Typically, 10×10^6 cells yielded $\sim 500 \mu\text{g}$ of cell lysate protein.

2.4 2-DE

EOS protein samples (200 μg for 11 cm and 350 μg for 18 cm IPG strips) were adjusted to 200 μL (11 cm strips) and 350 μL (18 cm strips) with DeStreak rehydration buffer and buffer/ampholyte added to give a final concentration of 0.5%. The mixtures were microcentrifuged at 2000 rpm for 2 min. IEF

was performed with a multi-sample IPGphor (GE Healthcare). Different pH gradient IPG strips were investigated. Paper wicks were placed over each electrode of the ceramic strip holders and 8 μL of Milli-Q H₂O was added to the wicks just prior to the addition of sample/DeStreak buffer mixtures. Dry IPG strips were added to each sample mixture with the gel side of the strip facing down and the strips were covered with mineral oil. The strip holders were placed in an IPGphor IEF cell and focused at 20°C with the following protocols: for 11 cm IPG strips: 50 V for 11 h (active rehydration), 250 V gradient for 1 h, 500 V gradient for 1 h, 1000 V gradient for 1 h, 8000 V gradient for 2 h, and held at 8000 V for 6 h; for 18 cm IPG strips: 50 V for 11 h, 250 V for 1 h, 500 V for 1 h, 1000 V for 1 h, 8000 V for 2 h, and held at 8000 V for 8 h. IPG strips were then removed and carefully blotted with damp filter paper to remove excess mineral oil. After IEF the strips were equilibrated for 15 min in 4 mL of an equilibration buffer (50 mM Tris-HCl, pH 8.8, containing 6 M urea, 2% SDS, 20% glycerol and 10 $\mu\text{L}/\text{mL}$ tri-(2-carboxyethyl) phosphine), followed by 15 min of equilibration with 4 mL of the above buffer containing 25 mg iodoacetamide/mL buffer. Strips were then rinsed with 1 \times Tris-glycine-SDS second dimension electrophoresis running buffer, pH 8.3, and placed in IPG wells of gels with the positive end of the strip toward the left side of the gels. Strips were subsequently overlaid with 0.5% molten agarose. Criterion gels were then placed in a second dimension electrophoresis cell and electrophoresis was conducted using pre-chilled 1 \times electrophoresis running buffer and 150 V for about 2 $\frac{1}{4}$ h or until the bromophenol blue dye reached the gel bottom. The electrophoresis (10°C) protocol for the Protean II gels was as follows: 35 V for 30 min, 50 V for 1 h, 70 V for 1 h, 100 V for 2 h, and 120 V for 12 h or until the dye front reached the bottom of the gel. After the second dimension of electrophoresis the gels were removed from their plates and rinsed with Milli-Q H₂O prior to staining.

2.5 Fluorescent staining of 2-D gels

Gels were fixed, stained, and destained essentially according to the manufacturer's (Invitrogen) recommendations. Briefly, gels intended for Pro-Q Diamond staining were fixed in a solution of 50% methanol and 10% acetic acid in double distilled H₂O overnight with shaking at RT then washed 3 \times in double distilled H₂O, stained in Pro-Q Diamond stain at RT for 90 min, and destained in a solution of 20% ACN, 50 mM sodium acetate (pH 4.0) in double distilled H₂O. Gels intended for Sypro Ruby staining were fixed in 10% methanol, 7% acetic acid, in double distilled H₂O for 2 h at RT. Subsequently, the Sypro Ruby stain was applied overnight at RT followed by destaining (10% ethanol) for 1 h. Some gels underwent both staining processes first with Pro-Q Diamond followed by Sypro Ruby.

2.6 Imaging of 2-D gels

Sypro stained gels were imaged at 100 μm resolution with a ProExpress 2-D Proteomic Imaging System (PerkinElmer Life and Analytical Sciences, Waltham, MA, USA) at 460/80 nm excitation and 650/150 nm emission wavelengths. Pro-Q Diamond stained gels were imaged with a Fuji FLA-5100 (Fujifilm USA, Valhalla, NY, USA) at 532 nm excitation (laser) and 575 nm longpass emission.

2.7 2-D gel image analysis

2-DE gel images were analyzed using Progenesis SameSpots software v2.0 (Nonlinear USA, Durham, NC). This software automatically detects individual protein spots within each image and matches identical protein spots across all images. It also removes noise from measurements of spot volumes using a proprietary algorithm for noise determination and correction. After automatic matching, manual review and adjustments were done to confirm proper spot detection and matching. The intensity of each protein spot was normalized based on the total spot volume of each gel, that is, the spot volume of each spot area was divided by the sum of all spot volumes in the gel. Spots present on less than two gels or with normalized volumes less than 150 were filtered out. Selected spots were robotically picked (Genomic Solutions, Ann Arbor, MI), trypsin digested, and robotically processed (Genomic Solutions) according to the manufacturer's recommendations prior to protein ID by MALDI-MS. Tryptic peptide samples were robotically transferred to MALDI-MS target plates. About 1 μL of MALDI matrix solution (CHCA in 50:50 ACN/H₂O, 5 mg/mL) was also added robotically to the tryptic samples.

2.8 Manual gel sample preparation for MS

When many protein spots were to be picked, we employed the Genomic Solutions robotics instrumentation (see Section 2.7). However, for those gels with few spots to be picked we used the following manual procedure. Gel samples were cut into 1 mm size pieces and placed into separate 0.5 mL polypropylene tubes. Ammonium bicarbonate buffer (100 μL of 50 mM, pH 8.0) was added to each tube and the samples were then incubated at 37°C for 30 min. After incubation, the buffer was removed and 100 μL of H₂O was added to each tube. The samples were then incubated again at 37°C for 30 min. After incubation, the H₂O was removed and 100 μL of ACN was added to each tube to dehydrate the gel pieces. The samples were vortexed and after 5 min the ACN was removed. ACN (100 μL) was again added to each of the sample tubes, vortexed, and ACN removed after 5 min. The samples were then placed in a speedvac for 45 min to remove any excess solvent. To a 20 μg vial of lyophilized trypsin (Promega, Madison, WI, USA) was added 2 mL of 25 mM ammonium

bicarbonate (pH 8.0). The trypsin solution was then vortexed and added to each sample tube in an amount required to just cover the dried gel (about 10 μL) and the samples were subsequently incubated at 37°C for 6 h. After digestion, the samples were removed from the oven and 1 μL of sample solution was spotted directly onto a MALDI target plate and allowed to dry. Subsequently, 1 μL of CHCA matrix solution (50:50 ACN/H₂O at 5 mg/mL) was applied on the sample spot and allowed to air dry.

2.9 MS

MALDI TOF/MS was used to analyze tryptic peptide samples and identify proteins. Data were acquired with an Applied Biosystems (Foster City, CA, USA) 4800 MALDI-TOF/TOF Proteomics Analyzer. Applied Biosystems software package included the 4000 Series Explorer (v3.6 RC1) with Oracle Database Schema (v3.19.0), and Data v3.80.0 to acquire both MS and MS/MS spectral data. The instrument was operated in positive ion reflectron mode with a mass range of 850–3000 Da and with the focus mass set at 1700 Da. For MS data, 1000–2000 laser shots were acquired and averaged from each sample spot. Automatic external calibration was performed using a peptide mixture with reference masses 904.468, 1296.685, 1570.677, and 2465.199. Following MALDI-MS analysis, MALDI-MS/MS was performed on several (5–10) of the most abundant ions from each sample spot. A 1 kV positive ion MS/MS method was used to acquire data under post-source decay conditions. The instrument precursor selection window was ± 3 Da. For MS/MS data, 2000 laser shots were acquired and averaged from each sample spot. Automatic external calibration was performed using reference fragment masses of 175.120, 480.257, 684.347, 1057.475, and 1441.635 (from precursor mass 1570.700). Applied Biosystems GPS ExplorerTM (v3.6) software was used in conjunction with MASCOT (Matrix Science, London, UK) to search the respective protein databases using both MS and MS/MS spectral data for protein ID. Protein match probabilities were determined using expectation values and/or MASCOT protein scores. The expectation value is the number of matches with equal or better scores that are expected to occur by chance alone. The default significance threshold was typically $p < 0.05$; however, for protein IDs herein we used a more stringent threshold of 10^{-3} . The lower the expectation value, the more significant the score. Expectation values were derived from Mascot scores (see www.matrixscience.com). MS peak filtering included the following parameters: mass range 800–4000 Da, minimum S/N filter = 10, mass exclusion list tolerance = 0.5 Da, and mass exclusion list (for some trypsin and keratin-containing compounds) included masses 842.51, 870.45, 1045.56, 1179.60, 1277.71, 1475.79, and 2211.1. For MS/MS peak filtering, the minimum S/N filter was set to 10. For protein ID, the human taxonomy was searched in either the NCBI or SwissProt databases. Other parameters included the

following: selecting trypsin; maximum missed cleavages = 1; fixed modifications included carbamidomethyl (C) for 2-D gel analyses only; variable modifications included oxidation (M); precursor tolerance was set at 0.2 Da; MS/MS fragment tolerance was set at 0.3 Da; mass = monoisotopic; and peptide charges were only considered as +1.

3 Results

3.1 General characterization of the expression data set

A representative 2-DE separation of an EOS whole cell lysate sample is shown in Fig. 1. The identities of selected non-redundant prominent protein spots are indicated in Table 1. Examples of 2-D gels focused over the pH ranges 3–10, 4–7, 5–8, and 6–11 are shown in Fig. 2. In general, EOS lysates focused reasonably well in the pH range 3–10. To demonstrate gel-to-gel reproducibility five gels were selected and the log of normalized spot volumes from gel 1 was plotted pairwise *versus* gels 2–5 as shown in Fig. 3 and the Pearson's

correlation co-efficient (r^2) was calculated. As evident in Fig. 3, the r^2 values indicated that the 2-DE analyses were reasonably reproducible as conducted (mean \pm SD = 0.91844 ± 0.01490). The distribution of proteins identified in the various fractions analyzed (subcellular, IEF, and total lysate) is given in Table 2. Overall, some 3141 proteins from the 2-DE gels were identified by MALDI-TOF/MS from fractions summarized in Table 2. All of these 3141 protein spots gave protein IDs with an expectation score of $< 10^{-3}$. Of these, 426 proteins identified had unique non-redundant SwissProt identifiers and 231 proteins of the 426 were classified as novel proteins not previously reported to be expressed in EOSs (Table 1). In general, the fractionation of proteins into the four commercially designated subcellular fractions shown using the ProteoExtract Subcellular Proteome Extraction procedure was quite useful even though some proteins did not distribute authentically; *i.e.* some proteins distributed correctly according to their known literature localization whereas other proteins did not. For example, many granular proteins (*e.g.* EPO, ECP, EDN, and MBP) distributed into the cytoskeletal fraction (F4) and most of the actin was in the nuclear fraction (F3). However, in general, the subcellular fractionation method

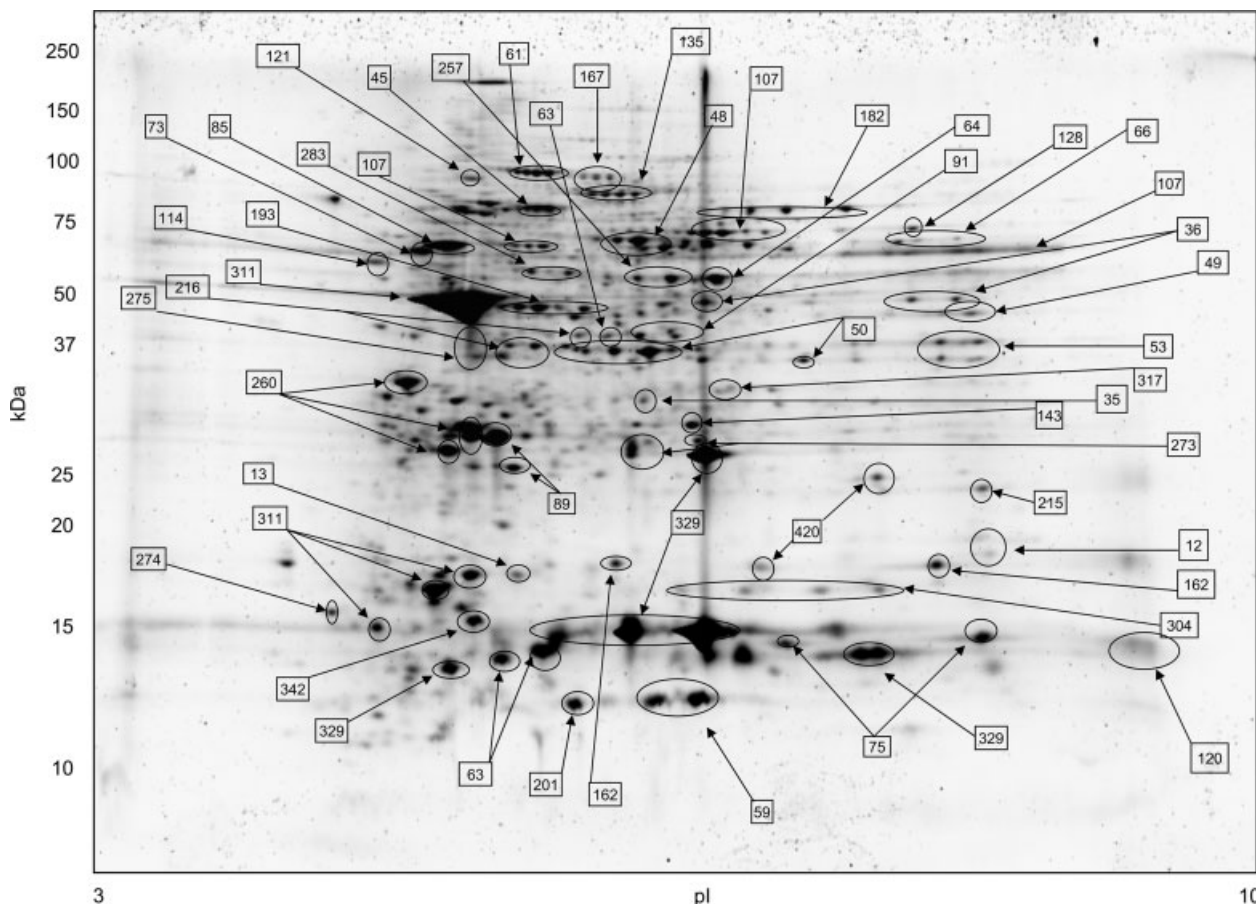


Figure 1. The proteome map of human peripheral blood EOSs. IEF was conducted in the pH range 3–10 in the first dimension. Major protein spots indicated by arrows are identified in Table 1. Protein vertical streak was due to galectin-10 insolubility (see Section 4). A total of 200 μ g EOS cell lysate was loaded to the gel.

Table 1. List of MS identified EOS proteins with significant SwissProt IDs

ID no. ^{a)}	Protein name	SwissProt Access. no. ^{b)}	Theoret./observ. pI ^{c)}	Theoret./observ. Mr ^{d)} (kDa)	Pept. match. (n)	Seq. cov. ^{e)} (%)	Mascot expect. score ^{f)}	Sub. cell. fract. no. ^{g)}
1*	Actin capping protein	A4D0V4	ND ^{h)}	ND	ND	ND	8.70E-19	6
2*	AH receptor-interacting protein	O00170	6.09/6.44	38.10/64.84	11	39	1.50E-06	6
3*	Hunc18b2	O00184					4.40E-08	2
4*	26S proteasome non-ATPase regulatory subunit 11	O00231	6.09/6.39	47.72/85.60	4	10	4.90E-03	3
5	Chloride intracellular channel	O00299	5.09/5.68	27.25/53.71	5	19	6.90E-04	5
6*	26S proteasome non-ATPase regulatory subunit 14	O00487	6.06/6.34	34.73/68.86	8	35	2.70E-04	3
7	Lysosomal- α -mannosidase precursor	O00754	6.84/5.95	114.36/97.37	13	15	2.70E-28	4
8*	Proteasome subunit- α -type 7	O14818	8.60/8.50	28.04/58.91	11	50	2.90E-16	5
9*	Ras-related protein Rab-7L1	O14966	6.73/6.66	23.43/40.18	9	52	2.20E-03	3
10*	Actin-related protein 2/3 complex subunit 1B	O15143	8.69	41.72	6	22	9.98E-05	6
11	Actin-related protein 2/3 complex subunit 2	O15144	6.84/6.90	34.43/57.04	22	63	5.80E-48	3
12*	Actin-related protein 2/3 complex subunit 3	O15145	8.82/8.49	20.76/28.61	7	35	1.90E-06	1
13*	Actin-related protein 2/3 complex subunit 5	O15511	5.47/5.87	16.37/27.15	7	56	1.30E-17	3
14*	Thioredoxin-like protein 1	O43396	4.84/5.50	32.63/68.45	11	50	1.30E-11	3
15*	Mitotic checkpoint protein	O43684	6.36/6.68	37.59/70.09	15	46	2.90E-19	2
16*	α -Actinin-4	O43707	5.27/5.72	105.24/184.80	35	46	1.20E-29	3
17	Keratin, type II cuticular Hb6	O43790	5.56/6.24	55.12/215.17	22	48	2.70E-16	1
18*	Glia maturation factor- γ	O60234	5.18/5.48	16.96/28.19	11	58	1.50E-23	1
19*	Sorting nexin-3	O60493	8.73/8.41	18.81/24.55	9	51	1.10E-04	5
20	Docking protein 2	O60496	6.58/5.93	45.75/84.31	16	32	2.10E-18	2
21*	Protein diaphanous homolog-1	O60610	ND	ND	ND	ND	4.80E-03	6
22	Mannose-6-phosphate receptor-binding protein-1	O60664	ND	ND	ND	ND	6.10E-11	6
23*	Histone H2B type 1-K	O60814	10.32/9.09	13.75/27.17	7	53	2.70E-15	3
24	WD repeat protein-1	O75083	6.18/6.60	66.84/126.16	16	40	4.30E-18	3
25*	Copine-3	O75131	5.60/5.98	60.95/112.67	14	26	1.20E-13	1
26	SH3 domain-binding glutamic acid-rich-like protein	O75368	5.22/5.79	12.76/20.10	3	35	3.20E-04	1
27	Citrate synthase, mitochondrial precursor	O75390	8.45/8.20	51.91/71.91	12	20	2.30E-34	4
28*	Protein CREG1 precursor	O75629	7.05/6.61	24.17/39.66	3	15	1.90E-03	4
29*	Protein XRP2	O75695	5.00/5.41	40.47/73.37	12	30	3.60E-06	3
30*	6-Phosphogluconolactonase	O95336	5.70/6.09	27.81/52.24	14	37	1.80E-35	1
31*	Ras-related protein Rab-3D	O95716	4.76/5.01	24.48/46.39	14	49	5.80E-13	3
32	L-Lactate dehydrogenase A chain	P00338	8.44/6.11	36.95/106.74	14	33	2.10E-17	5
33	Glutamate dehydrogenase 1, mitochondrial precursor	P00367	7.66/7.01	61.70/95.99	14	29	2.90E-11	3
34	Glutathione reductase, mitochondrial precursor	P00390	8.74	56.79	14	34	1.26E-29	6
35*	Purine nucleoside phosphorylase	P00491	6.45/6.57	32.33/58.66	14	75	5.80E-45	5
37	Carbonic anhydrase 1	P00915	6.59/8.34	28.91/71.39	14	58	3.40E-28	4
38*	Carbonic anhydrase 2	P00918	6.87/7.13	29.28/58.26	14	40	2.70E-12	1
39	α -1-Antitrypsin precursor	P01009	5.37/5.40	46.88/89.30	14	21	1.20E-07	1
40	α -1-Antichymotrypsin precursor	P01011	5.33/4.77	47.49/111.08	14	30	3.60E-09	3
41	Hemoglobin subunit- δ	P02042	7.85/8.67	16.16/16.71	14	95	8.50E-23	4
42	Spectrin- α -chain, erythrocyte	P02549	4.96/5.37	280.88/219.26	14	15	1.30E-04	1
43	Fibrinogen- β -chain precursor	P02675	8.54	56.58	14	43	2.51E-14	6
44	Transthyretin precursor	P02766	5.52/6.13	15.99/25.35	14	63	5.80E-13	3

Table 1. Continued

ID no. ^{a)}	Protein name	SwissProt Access. no. ^{b)}	Theoret./observ. p/ ^{c)}	Theoret./observ. Mr ^{d)} (kDa)	Pept. match. (n)	Seq. cov. ^{e)} (%)	Mascot expect. score ^{f)}	Sub. cell. fract. no. ^{g)}
45	Serum albumin precursor	P02768	5.92/6.30	71.32/34.20	14	34	9.20E-28	2
46	Lactotransferrin precursor	P02788	8.50/7.16	80.01/167.43	14	61	1.50E-89	3
47*	Ferritin light chain	P02792	5.51/5.97	20.06/93.00	14	46	1.30E-30	3
48	Catalase	P04040	6.95/6.73	59.82/118.28	14	29	2.10E-64	6
49	Fructose-bisphosphate aldolase-A	P04075	8.39/8.45	39.85/73.95	14	36	1.10E-12	5
50	Annexin-A1	P04083	6.64/6.39	38.92/66.84	14	70	2.10E-92	1
51	Superoxide dismutase [Mn], mitochondrial precursor	P04179	8.35/6.15	24.88/42.73	14	16	1.90E-03	4
52*	Keratin, type II cytoskeletal-1	P04264	8.16/6.09	66.02/53.75	14	32	5.40E-49	5
53	Glyceraldehyde-3-phosphate dehydrogenase	P04406	8.58/8.52	36.21/57.25	14	57	8.50E-14	5
54*	Calpain small subunit 1	P04632	5.05/5.29	28.47/51.56	14	30	7.30E-09	3
55	Cytochrome b-245 heavy chain	P04839	8.90/7.20	66.21/26.85	14	17	1.30E-05	4
56	Guanine nucleotide-binding protein G(i), α -2 subunit	P04899	ND	ND	ND	ND	2.20E-45	6
57	Aldehyde dehydrogenase, mitochondrial precursor	P05091	6.63/7.06	56.86/62.30	15	30	2.30E-35	4
58	Integrin- β -2 precursor	P05107	6.69/6.22	87.98/88.07	29	39	2.70E-23	4
59	Protein S100-A8	P05109	6.51/6.39	10.85/45.31	10	82	1.80E-20	5
60	Myeloperoxidase precursor	P05164	9.19/9.75	84.78/90.76	23	31	3.60E-24	5
61	Gelsolin precursor	P06396	5.90/6.32	86.04/131.40	21	29	1.50E-52	5
62	ATP synthase subunit- β , mitochondrial precursor	P06576	5.26/5.40	56.52/95.54	20	52	1.20E-59	3
63	Protein S100-A9	P06702	5.71/8.70	13.29/282.65	6	50	5.80E-22	5
64	α -Enolase	P06733	6.99/5.82	47.48/145.56	18	44	8.50E-15	5
65	Glycogen phosphorylase, liver form	P06737	6.71/6.84	97.49/184.17	32	41	6.80E-50	5
66	Glucose-6-phosphate isomerase	P06744	8.43/8.23	63.34/101.91	25	51	2.10E-32	5
67	Tropomyosin- α -3 chain	P06753	ND	ND	ND	ND	3.00E-33	6
68	L-Lactate dehydrogenase B chain	P07195	5.72/6.02	36.90/62.40	14	47	6.80E-24	1
69	Glutathione peroxidase-1	P07203	6.15/5.97	22.27/36.59	10	69	7.30E-11	2
70	Protein disulfide-isomerase precursor	P07237	4.76/5.17	57.48/107.61	25	57	5.80E-79	3
71	Cathepsin-D precursor	P07339	6.10/5.98	45.04/52.24	14	40	2.90E-15	1
72*	Annexin-A2	P07355	7.57/7.62	38.81/72.03	19	49	2.70E-26	1
73	Tubulin- β -2 chain	P07437	4.78/5.29	50.10/97.65	22	55	8.50E-28	3
74	β -Hexosaminidase- β -chain precursor	P07686	6.29	63.53	11	19	9.98E-05	6
75	Profilin-1	P07737	8.48/8.53	15.22/25.17	9	62	4.30E-52	3
76*	Adenine phosphoribosyltransferase	P07741	5.78/5.66	19.77/34.90	6	32	5.40E-24	3
77*	HSP-90- α	P07900	ND	ND	ND	ND	3.50E-42	6
78*	Heterogeneous nuclear ribonucleoproteins C1/C2	P07910	4.95/8.19	33.71/65.31	7	25	5.50E-03	2
79	HSP-170 kDa	P08107	5.48/6.18	70.29/78.53	17	26	2.30E-47	5
80	Annexin A6	P08133	5.42/6.02	76.17/132.77	41	65	6.80E-63	3
81	β -Glucuronidase precursor	P08236	6.54/6.94	75.01/132.90	9	24	8.00E-03	1
82*	HSP-90- β	P08238	4.97/5.38	83.55/154.23	24	35	1.10E-20	1
83	Leukocyte elastase precursor	P08246	9.71/5.65	29.13/70.56	7	34	2.30E-07	3
84*	Glutathione S-transferase A1	P08263	ND	ND	ND	ND	6.10E-18	6
85	Vimentin	P08670	5.06/5.24	5.38/86.36	25	57	6.80E-29	5
86*	Guanine nucleotide-binding protein G(k) subunit- α	P08754	ND	ND	ND	ND	2.60E-03	6
87*	Annexin A5	P08758	4.94/5.40	35.97/63.04	18	57	6.80E-79	3

Table 1. Continued

ID no. ^{a)}	Protein name	SwissProt Access. no. ^{b)}	Theoret./observ. p/ ^{c)}	Theoret./observ. Mr ^{d)} (kDa)	Pept. match. (n)	Seq. cov. ^{e)} (%)	Mascot expect. score ^{f)}	Sub. cell. fract. no. ^{g)}
88*	40S Ribosomal protein SA	P08865	4.79/5.11	32.95/75.93	10	45	1.30E-14	3
89	Glutathione S-transferase P	P09211	5.43/6.01	23.44/37.00	11	53	5.40E-53	1
90	High mobility group protein-B1	P09429	5.62/6.56	25.05/57.42	11	46	1.10E-36	3
91*	Fructose-1,6-bisphosphatase 1	P09467	6.54/6.75	37.19/74.75	20	54	1.30E-65	3
92	Annexin-A4	P09525	5.84/5.97	36.09/61.14	22	63	6.80E-57	1
93*	Heterogeneous nuclear ribonucleoprotein-A1	P09651	9.26/9.08	38.81/51.48	15	46	3.40E-11	5
94*	U2 small nuclear ribonucleoprotein-A	P09661	8.72/8.52	28.51/44.45	8	28	7.80E-04	6
95	Leukotriene A-4 hydrolase	P09960	5.80/6.23	69.87/125.95	27	51	1.70E-34	1
96*	Histone H2A.Z	P0C0S5	10.58/5.63	35.67/25.67	2	12	4.40E-06	3
97	EDN	P10153	9.10/8.89	18.86/28.78	5	22	2.30E-24	1
98*	Lysosomal- α -glucosidase precursor	P10253	5.62/5.89	106.13/41.83	13	15	1.00E-03	4
99	Thioredoxin	P10599	4.82/5.31	12.01/17.70	8	55	5.40E-11	1
100*	Lysosomal protective protein precursor	P10619	6.16/5.20	54.94/55.37	8	14	9.20E-13	5
101	Esterase-D	P10768	6.54/6.57	31.96/56.58	11	49	7.30E-14	1
102	78 kDa Glucose-regulated protein precursor	P11021	ND	ND	ND	ND	3.00E-38	6
103	71 kDa Cognate HSP	P11142	5.37/5.85	71.08/142.38	22	35	9.20E-62	3
104	Integrin- α -M precursor	P11215	6.88/6.85	128.41/234.21	30	56	1.83E-21	4
105*	Medium-chain-specific acyl-CoA dehydrogenase, mitochondrial precursor	P11310	8.61/6.84	47.01/80.06	13	35	7.30E-11	3
106	Glucose-6-phosphate-1-dehydrogenase	P11413	6.39/6.88	59.68/112.14	32	70	2.90E-28	3
107	EPO precursor	P11678	10.31/7.62	81.96/113.08	13	18	4.60E-07	6
108	Proliferating cell nuclear antigen	P12004	4.57/5.12	29.09/64.84	7	31	3.80E-05	3
109	Annexin-A3	P12429	5.63/8.74	36.52/68.97	10	36	1.10E-37	4
110	ECP precursor	P12724	10.31/9.53	18.94/35.5	7	42	1.20E-20	3
111	α -Actinin-1	P12814	5.25	103.56	25	35	1.50E-14	2
112	Myosin heavy chain, cardiac muscle- β -isoform	P12883	5.63/3.60	223.76/32.64	17	13	3.00E-03	6
113*	ATP-dependent DNA helicase-2-subunit 1	P12956	6.23/6.59	70.08/135.42	22	49	8.50E-42	3
114	Ribonuclease inhibitor	P13489	4.71/5.11	51.77/85.58	21	62	5.40E-56	1
115*	Elongation factor-2	P13639	ND	ND	ND	ND	1.40E-16	6
116*	Keratin, type I cytoskeletal 10	P13645	5.13/7.93	59.711/50.00	19	29	7.30E-33	3
117*	Protein disulfide-isomerase A4 precursor	P13667	4.96/5.51	73.23/143.51	34	48	5.80E-46	3
118	Translationally controlled tumor protein	P13693	4.84/5.25	19.70/39.23	10	47	1.50E-19	1
119	δ -Aminolevulinic acid dehydratase	P13716	6.32/6.57	36.73/70.58	11	34	5.50E-09	3
120	Bone marrow proteoglycan precursor	P13727	6.23/9.39	25.90/20.82	6	26	1.10E-14	1
121	Plastin-2 (L-plastin)	P13796	5.20/5.63	70.82/121.32	30	57	5.40E-56	1
122	Acylamino-acid-releasing enzyme	P13798	5.29/5.71	82.14/152.88	19	31	4.60E-18	3
123	Macrophage migration inhibitory factor	P14174	8.24/7.90	12.64/18.94	5	24	2.70E-11	1
124	Hematopoietic lineage cell-specific protein	P14317	4.74/7.11	50.08/73.33	8	17	2.20E-04	6
125*	Farnesyl pyrophosphate synthetase	P14324	ND	ND	ND	ND	1.70E-08	6
126*	Alcohol dehydrogenase [NADP+]	P14550	6.32/6.66	36.89/71.94	18	55	3.40E-40	1
127	Neutrophil cytosol factor-1	P14598	9.12/7.87	44.88/101.38	11	31	7.30E-21	6
128	Pyruvate kinase isozymes M1/M2	P14618	7.96/7.90	58.47/104.26	19	42	5.40E-13	1
129	Endoplasmin precursor	P14625	4.76/5.21	92.67/180.61	28	38	3.60E-56	3

Table 1. Continued

ID no. ^{a)}	Protein name	SwissProt Access. no. ^{b)}	Theoret./observ. p/ ^{c)}	Theoret./observ. M _r ^{d)} (kDa)	Pept. match. (n)	Seq. cov. ^{e)} (%)	Mascot expect. score ^{f)}	Sub. cell. fract. no. ^{g)}
130	Heterogeneous nuclear ribonucleoprotein L	P14866	6.65/6.86	60.72/122.75	12	27	4.60E-08	3
131	Aspartyl-tRNA synthetase, cytoplasmic	P14868	6.11	57.5	22	44	9.98E-24	6
132*	Ras-related C3 botulinum toxin substrate-2-precursor	P15153	7.52/7.87	21.81/37.71	8	39	3.60E-44	1
133	Ezrin	P15311	5.94	69.48	20	30	3.15E-19	6
134	Nucleoside diphosphate kinase-A	P15531	5.83/6.16	17.31/29.25	6	42	1.80E-16	1
135	Arachidonate-15-lipoxygenase	P16050	6.14/6.58	75.50/114.56	21	40	3.40E-19	1
136*	Histone H2A.x	P16104	10.74/5.55	15.14/27.56	4	48	5.80E-04	3
137*	Carbonyl reductase [NADPH]-1	P16152	8.55/9.67	30.64/49.27	8	41	2.00E-04	6
138	β-Galactosidase-related protein precursor	P16279	6.5/6.23	60.86/123.48	11	24	4.60E-11	3
139*	Stathmin	P16949	5.76/6.01	17.29/28.28	9	42	2.10E-26	3
140	Galectin-3	P17931	8.61/8.20	26.23/57.44	5	22	4.30E-03	1
141*	T-complex protein-1-subunit-α	P17987	ND	ND	ND	ND	3.90E-04	6
142	Vinculin	P18206	5.50/6.47	124.29/176.11	38	36	1.30E-32	1
143	Phosphoglycerate mutase-1	P18669	6.67/6.54	28.90/53.87	14	56	4.30E-31	1
144*	Myosin regulatory light chain-2, nonsarcomeric	P19105	4.67/5.04	19.84/30.71	9	63	1.70E-23	2
145	Neutrophil cytosol factor-2	P19878	5.88/6.22	60.24/119.95	21	42	9.20E-23	1
146*	Annexin-A7	P20073	5.52/6.26	52.99/86.00	10	23	2.30E-09	1
147	Azurocidin precursor	P20160	9.75/9.47	27.32/57.23	5	30	1.70E-13	3
148*	Proteasome subunit-β-type 1	P20618	8.27/7.84	26.70/43.24	10	52	2.90E-17	3
149	Lamin-B1	P20700	ND	ND	ND	ND	1.70E-21	6
150*	Vacuolar ATP synthase subunit B, brain isoform	P21281	5.57/6.03	56.81/101.80	10	25	1.80E-08	3
151*	Iron-responsive element-binding protein-1	P21399	ND	ND	ND	ND	1.40E-06	6
152*	Voltage-dependent anion-selective channel protein-1	P21796	8.62/5.30	30.87/51.41	9	41	2.10E-19	4
153*	Ubiquitin-like modifier-activating enzyme-1	P22314	5.49/5.74	118.86/171.81	29	40	7.30E-30	1
154	Nucleoside diphosphate kinase-B	P22392	8.52/8.39	17.40/26.76	13	87	2.30E-28	1
155	Heterogeneous nuclear ribonucleoproteins-A2/B1 precursor	P22626	8.97/7.79	37.46/45.38	16	42	3.60E-30	3
156	Cytochrome b-c1 complex subunit-2, mitochondrial precursor	P22695	8.74/7.67	48.58/81.54	9	30	4.60E-06	3
157	Liver carboxylesterase-1 precursor	P23141	6.15/6.11	62.77/95.84	13	26	2.80E-05	4
158	Splicing factor, proline- and glutamine-rich	P23246	9.45/7.89	76.21/228.51	9	17	2.90E-20	6
159	Peptidyl-prolyl cis-trans isomerase B precursor	P23284	9.33/9.23	22.79/25.86	7	41	1.80E-09	6
160*	Tryptophanyl-tRNA synthetase	P23381	5.83/6.25	53.47/98.77	18	50	4.30E-24	1
161*	Adenosylhomocysteinase	P23526	5.92/6.28	48.26/80.14	20	43	2.10E-36	1
162	Cofilin-1	P23528	8.22/8.13	18.72/28.60	10	65	3.40E-26	1
163	Myeloblastin precursor	P24158	8.72/9.04	28.25/25.26	3	11	4.60E-14	4
164	Proteasome subunit-α-type 1	P25786	6.15/6.45	29.82/61.79	10	47	2.90E-16	3
165	Proteasome subunit-α-type 2	P25787	6.92/6.82	26.00/45.64	13	61	1.70E-34	3
166*	Proteasome subunit-α-type 4	P25789	7.57/7.57	29.75/59.21	13	59	4.60E-33	3
167	Moesin	P26038	6.08/6.51	67.89/150.87	30	50	4.30E-51	3
168*	Protein S100-A4	P26447	5.85/5.87	11.95/13.94	6	36	2.90E-17	1
169*	Elongation factor 1-γ	P26641	6.25	50.43	15	33	3.97E-36	6
170*	Annexin-A13	P27216	5.47/5.71	35.54/65.47	8	30	3.00E-04	3
171*	14-3-3 Protein theta	P27348	ND	ND	ND	ND	1.50E-08	6

Table 1. Continued

ID no. ^{a)}	Protein name	SwissProt Access. no. ^{b)}	Theoret./observ. p/ ^{c)}	Theoret./observ. M _r ^{d)} (kDa)	Pept. match. (n)	Seq. cov. ^{e)} (%)	Mascot expect. score ^{f)}	Sub. cell. fract. no. ^{g)}
172	Replication protein A 70kDa	P27694	6.92/6.93	68.72/144.08	14	30	5.80E-07	3
173	Calreticulin precursor	P27797	4.29/4.77	48.28/134.58	14	44	4.60E-40	3
174*	Histone H2A type 1-E	P28001	11.05/6.25	14.10/26.03	7	43	3.40E-20	3
175*	Proteasome subunit-β-type 8 precursor	P28062	7.63/8.11	30.68/56.66	10	29	2.30E-30	3
176	Proteasome subunit-β-type 9 precursor	P28065	4.93/5.25	23.36/38.82	7	40	3.80E-05	3
177*	Proteasome subunit-α-type 5	P28066	4.74/5.18	26.57/55.00	8	43	3.50E-06	3
178	Proteasome subunit-β-type 4 precursor	P28070	5.72/5.93	29.23/51.19	7	37	1.50E-16	3
179	Mitogen-activated protein kinase-1	P28482	6.53/6.73	41.76/76.16	5	15	6.80E-08	3
180*	Grancalcin	P28676	5.02/5.23	24.22/47.52	10	52	2.90E-18	3
181	Tyrosine-protein phosphatase non-receptor type-6	P29350	7.65/6.32	67.92/101.19	15	33	7.30E-34	3
182	Transketolase	P29401	7.58/7.41	68.52/144.42	14	25	2.30E-58	6
183*	Endoplasmic reticulum protein ERp29 precursor	P30040	6.77/6.53	29.03/61.97	11	36	7.30E-41	3
184	Peroxiredoxin-6	P30041	6.02/6.49	25.13/40.62	5	21	3.00E-04	1
185	Flavin reductase	P30043	7.13/7.48	22.22/42.00	10	67	1.30E-30	1
186	Peroxiredoxin-5, mitochondrial precursor	P30044	8.85/7.04	23.00/27.77	11	49	4.60E-26	1
187	Thioredoxin-dependent peroxide reductase, mitochondrial precursor	P30048	7.67/6.06	28.02/35.25	5	21	5.80E-21	2
188*	UMP-CMP kinase	P30085	5.44/5.82	22.44/37.00	9	58	2.90E-08	1
189*	Phosphatidylethanolamine-binding protein-1	P30086	7.42/7.63	21.16/35.70	13	67	6.80E-34	1
190	Protein disulfide-isomerase A3 precursor	P30101	5.98/5.95	57.46/108.29	26	49	1.80E-60	3
191*	Ser/Thr-protein phosphatase 2A 65kDa	P30153	4.96/5.51	66.07/121.85	18	35	1.10E-16	3
192*	Ser/Thr Sorcin	P30626	5.32/5.49	21.95/33.15	7	40	3.60E-11	2
193	Ser/Thr Leukocyte elastase inhibitor	P30740	5.90/6.20	42.83/74.25	13	38	1.30E-05	2
194	Succinate dehydrogenase mitochondrial precursor	P31040	7.06/5.83	73.67/33.63	12	19	1.10E-05	4
195	Coronin-1A	P31146	6.25/6.76	51.68/98.51	14	32	5.40E-08	1
196	Rab GDP dissociation inhibitor-α	P31150	5.00/5.37	51.12/113.09	22	55	4.60E-22	3
197*	Heterogeneous nuclear ribonucleoprotein H3	P31942	6.37/5.73	36.96/69.00	6	26	1.80E-14	6
198	Heterogeneous nuclear ribonucleoprotein-H	P31943	5.89	49.48	10	33	3.15E-09	6
199	14-3-3 protein-β/α	P31946	4.76/4.09	28.05/59.13	8	32	5.60E-03	6
200*	Stress-induced-phosphoprotein-1	P31948	ND	ND	ND	ND	1.40E-04	6
201*	Protein S100-A11	P31949	6.51/7.33	10.88/15.94	9	60	5.40E-31	6
202	Peroxiredoxin-2	P32119	5.68/5.46	22.65/36.44	7	27	3.40E-22	2
203*	Cytidine deaminase	P32320	6.55/6.16	16.69/24.75	5	48	6.80E-06	2
204	N-acetylgalactosamine-6-sulfatase precursor	P34059	6.25/6.42	58.45/135.28	13	24	5.40E-26	4
205	Heat shock 70 kDa protein-4	P34932	5.18/5.22	95.10/175.14	17	20	3.60E-07	3
206*	Prohibitin	P35232	5.57/7.38	29.84/61.79	5	24	4.20E-03	4
207*	Keratin, type-I-cytoskeletal-9	P35527	5.19/5.72	62.32/122.35	15	35	1.20E-14	3
208*	Phosphoenolpyruvate carboxykinase, cytosolic [GTP]	P35558	ND	ND	ND	ND	8.70E-45	6
209	Myosin-9	P35579	5.50/5.51	227.65/214.11	33	23	2.10E-12	2
210	Myosin-11	P35749	5.42/5.77	228.05/131.40	25	16	3.10E-04	2
211*	Keratin, type-II-cytoskeletal-2-epidermal	P35908	8.07/6.14	66.11/43.76	12	22	2.90E-12	1
212*	Phosphoglucomutase-1	P36871	6.32/6.48	61.56/105.99	21	43	3.60E-20	1
213*	Phospholipid hydroperoxide glutathione peroxidase, mitochondrial precursor	P36969	8.64/7.50	22.68/29.12	11	60	9.20E-20	1

Table 1. Continued

ID no. ^{a)}	Protein name	SwissProt Access. no. ^{b)}	Theoret./observ. p/ ^{c)}	Theoret./observ. (kDa)	Pept. match. (n)	Seq. cov. ^{e)} (%)	Mascot expect. score ^{f)}	Sub. cell. fract. no. ^{g)}
214*	Hippocalcin-like protein-1	P37235	5.21/5.36	22.41/31.71	6	32	2.10E-05	1
215*	Transgelin-2	P37802	8.41/8.07	22.55/35.68	17	75	5.40E-35	1
216*	Transaldolase	P37837	6.36/5.89	37.69/63.54	18	45	2.30E-38	4
217*	Vacuolar ATP synthase catalytic subunit-A, ubiquitous isoform	P38606	5.35/5.72	68.66/137.78	15	32	6.80E-09	3
218*	Stress-70 protein, mitochondrial precursor	P38646	5.87/5.80	73.92/131.24	18	32	2.90E-37	3
219*	Eukaryotic initiation factor-4A-III	P38919	6.30/6.43	47.13/88.36	7	14	3.40E-12	3
220*	Acidic leucine-rich nuclear phosphoprotein-32	P39687	3.99/4.48	28.68/56.85	9	31	1.80E-18	3
221	Macrophage capping protein	P40121	5.88/6.17	38.78/75.25	11	43	2.30E-07	1
222	Malate dehydrogenase, cytoplasmic	P40925	ND	ND	ND	ND	6.90E-15	6
223	Malate dehydrogenase, mitochondrial precursor	P40926	8.92/9.11	35.96/61.23	13	50	1.50E-14	6
224	Myeloid cell nuclear differentiation antigen	P41218	9.77/7.92	46.09/111.49	8	23	1.80E-19	6
225	Tyrosine-protein kinase CSK	P41240	6.62/6.92	51.24/99.43	15	44	2.90E-10	3
226	Caspase-3 precursor	P42574	6.09/6.50	32.04/56.82	19	63	5.80E-21	2
227*	Lysosomal Pro-X carboxypeptidase precursor	P42785	6.75/6.47	56.28/109.73	14	26	2.30E-21	4
228*	Platelet-activating factor acetylhydrolase-1B-subunit- α	P43034	6.97	47.18	13	34	9.98E-25	6
229	Glycerol-3-phosphate dehydrogenase, mitochondrial precursor	P43304	7.23	81.3	20	26	3.97E-14	6
230	26S protease regulatory subunit 6B	P43686	ND	ND	ND	ND	4.00E-04	6
231*	Ubiquitin carboxyl-terminal hydrolase-5	P45974	4.91/5.42	96.64/168.41	19	25	3.60E-07	1
232*	Crk-like protein	P46109	6.26/6.47	33.87/67.18	14	57	7.30E-11	2
233	Vesicle-fusing ATPase	P46459	6.52	83.02	17	24	1.26E-07	6
234	F-actin capping protein subunit- β	P47756	5.36/5.88	31.62/57.61	19	65	2.10E-27	2
235*	26S proteasome non-ATPase regulatory subunit-8	P48556	6.85/6.51	30.16/52.13	11	33	4.30E-20	2
236	Serpin B10	P48595	5.80/5.97	45.49/241.04	21	59	3.60E-42	1
237*	Glutathione synthetase	P48637	ND	ND	ND	ND	5.50E-15	6
238*	T-complex protein-1-subunit epsilon	P48643	ND	ND	ND	ND	3.00E-04	6
239*	Keratin, type II cytoskeletal 6E	P48668	8.14/6.99	60.27/44.52	16	29	2.10E-09	2
240	Isocitrate dehydrogenase [NADP], mitochondrial precursor	P48735	8.88/6.53	51.33/116.03	20	47	1.50E-19	4
241*	CD97 antigen precursor	P48960	6.50/5.39	94.60/133.76	7	9	9.20E-07	2
242*	Calcium signal-modulating cyclophilin ligand	P49069	ND	ND	ND	ND	9.30E-06	6
243*	Ribose-5-phosphate isomerase	P49247	8.78/7.18	33.53/54.80	8	27	4.30E-11	1
244*	T-complex protein-1-subunit- γ	P49368	6.10/6.42	61.07/109.15	16	33	4.60E-12	2
245*	Elongation factor Tu, mitochondrial precursor	P49411	7.26	49.85	8	23	9.98E-06	6
246*	Proteasome subunit- β -type 3	P49720	6.14/6.31	23.22/48.25	11	50	1.50E-23	3
247*	Proteasome subunit- β -type 2	P49721	6.51	22.99	10	46	2.51E-19	6
248	Rab GDP dissociation inhibitor- β	P50395	6.11/6.37	51.09/82.02	30	73	9.20E-59	1
249*	Vasodilator-stimulated phosphoprotein	P50552	9.05/6.34	39.98/56.07	8	23	8.50E-11	4
250*	Dynamin-2	P50570	7.04/6.38	98.45/131.31	24	29	1.80E-18	3
251	Annexin-A11	P50995	7.53/8.48	54.68	24	41	1.50E-40	4
252*	Ras-related protein Rab-5C	P51148	8.64/5.23	23.70/56.07	9	44	4.40E-06	4
253*	Ras-related protein Rab-7	P51149	6.4	23.76	12	66	6.80E-37	3

Table 1. Continued

ID no. ^{a)}	Protein name	SwissProt Access. no. ^{b)}	Theoret./observ. p/ ^{c)}	Theoret./observ. M _r ^{d)} (kDa)	Pept. match. (n)	Seq. cov. ^{e)} (%)	Mascot expect. score ^{f)}	Sub. cell. fract. no. ^{g)}
254*	Ras-related protein Rab-27A	P51159	5.19/5.50	25.13/52.12	9	35	4.60E-10	2
255	Galactokinase	P51570	6.04/5.90	42.70/77.82	11	28	1.50E-38	6
256*	Heterogeneous nuclear ribonucleoprotein A3	P51991	9.10/9.66	39.80/63.97	11	31	8.80E-04	6
257	6-Phosphogluconate dehydrogenase	P52209	6.80/7.07	53.62/83.71	21	46	6.80E-51	1
258*	Heterogeneous nuclear ribonucleoprotein M	P52272	8.85/8.12	77.62/79.83	16	26	9.30E-04	6
259	Rho GDP-dissociation inhibitor 1	P52565	5.03/5.43	23.25/51.19	10	43	1.10E-32	3
260	Rho GDP-dissociation inhibitor 2	P52566	5.10/5.61	23.03/49.74	12	80	6.80E-19	3
261*	Hexokinase-3	P52790	5.27/5.57	100.51/166.43	20	26	2.30E-21	1
262	F-actin capping protein α -1 subunit	P52907	5.45/5.74	33.07/64.26	16	69	1.70E-15	2
263*	Biliverdin reductase A precursor	P53004	6.06/6.35	33.69/69.46	13	42	5.80E-34	1
264*	ATP-citrate synthase	P53396	6.95/7.17	121.66/214.05	34	39	9.20E-30	3
265	Dipeptidyl-peptidase 1 precursor	P53634	6.54/5.37	52.61/21.11	5	10	8.70E-05	3
266	Tyrosyl-tRNA synthetase, cytoplasmic	P54577	6.64/6.84	56.45/116.20	13	27	5.40E-10	3
267	Adenylate kinase isoenzyme 2, mitochondrial	P54819	7.85/8.25	26.69/55.06	9	41	8.50E-11	4
268*	α -Soluble NSF attachment protein	P54920	5.23/5.57	33.68/63.46	12	44	4.60E-12	3
269*	Transitional endoplasmic reticulum ATPase	P55072	ND	ND	ND	ND	6.60E-05	6
270*	Histone H2B type 1-D	P58876	10.32/9.56	13.98/27.17	7	52	1.10E-11	3
271	Neutrophil defensin-1-precursor	P59665	6.54/8.33	10.54/55.89	5	26	4.60E-17	4
272*	Actin-related protein 2/3 complex subunit-4	P59998	8.53/8.48	19.67/31.69	10	44	3.60E-16	3
273*	Triosephosphate isomerase	P60174	6.45/6.82	26.94/47.85	16	70	2.30E-42	1
274*	Myosin light polypeptide-6	P60660	4.56/3.51	16.96/18.16	10	62	4.30E-24	6
275	Actin, cytoplasmic-1	P60709	5.29/5.8	42.02/63.77	6	23	7.30E-21	2
276*	Eukaryotic initiation factor-4A-1	P60842	5.32/5.8	46.35/92.56	18	50	1.20E-09	3
277*	Ribose-phosphate pyrophosphokinase-I	P60891	6.56/6.94	35.33/68.86	8	28	1.70E-07	3
278	Proteasome subunit- α type 6	P60900	6.34/6.47	27.84/50.00	7	31	2.90E-09	3
279*	Cell division control protein-42 homolog precursor	P60953	5.76/6.85	21.70/34.13	6	29	9.20E-15	3
280	Dextrin	P60981	8.06/7.95	18.95/28.60	1	6	2.30E-03	3
281*	Ras-related protein Rab-2A	P61019	6.08/5.83	23.70/47.74	9	50	5.80E-11	3
282*	Ubiquitin-conjugating enzyme E2 N	P61088	6.13/6.22	17.18/25.71	11	57	9.20E-15	1
283	Actin-related protein-3	P61158	5.61/6.12	47.67/84.00	17	48	6.80E-40	1
284*	Actin-like protein-2	P61160	6.30/6.58	45.02/79.74	17	50	3.60E-17	3
285*	α -Centractin	P61163	6.19	42.7	12	37	1.80E-16	2
286*	ADP-ribosylation factor-3	P61204	6.84/7.07	20.46/56.97	11	69	5.40E-16	4
287*	Ras-related protein Rap-1b-precursor	P61224	5.65/5.82	21.04/57.68	8	43	1.50E-10	4
288	Transforming protein RhoA precursor	P61586	5.83/6.34	22.10/42.90	8	39	2.30E-11	1
289*	10 kDa HSP, mitochondrial	P61604	8.91/6.94	10.92/169.95	9	66	6.80E-26	4
290	Lysozyme C precursor	P61626	9.38/8.95	16.98/23.91	6	38	7.30E-12	1
291	β -2-Microglobulin precursor	P61769	6.06/6.43	13.82/28.62	3	37	3.40E-04	4
292*	Heterogeneous nuclear ribonucleoprotein K	P61978	5.39/5.88	51.30/107.85	14	34	1.80E-12	2
293	14-3-3 Protein- γ	P61981	4.8	28.46	9	36	3.40E-10	2
294*	Ser/Thr protein phosphatase- α -catalytic subunit	P62136	5.94/6.15	38.23/71.15	14	32	7.30E-18	3
295*	Ser/Thr protein phosphatase- β -catalytic subunit	P62140	5.84/6.18	37.69/72.20	17	58	1.30E-12	3
296	Calmodulin	P62158	4.09/3.38	16.70/23.48	5	45	1.10E-19	6

Table 1. Continued

ID no. ^{a)}	Protein name	SwissProt Access. no. ^{b)}	Theoret./observ. p/ ^{c)}	Theoret./observ. (kDa)	Pept. match. (n)	Seq. cov. ^{e)} (%)	Mascot expect. score ^{f)}	Sub. cell. fract. no. ^{g)}
297*	14-3-3 Protein epsilon	P62258	4.63	29.33	13	53	2.30E-18	3
298*	26S Protease regulatory subunit-S10B	P62333	7.1	44.43	12	35	5.00E-09	6
299*	Ras-related protein Rab-11A	P62491	3.12/8.88	24.49/28.69	9	33	4.90E-06	4
300	Histone-H4	P62805	11.36/9.50	11.36/24.82	7	56	3.40E-33	3
301	Histone-H2B type 1-C/E/F/G/I	P62807	10.31/8.47	13.98/26.16	9	61	4.30E-21	3
302*	GTP-binding nuclear protein Ran	P62826	7.01/7.14	24.57/43.15	15	56	1.70E-28	1
303*	Guanine nucleotide-binding protein G(I)/G(S)/G(T) subunit-β-2	P62879	5.60/5.87	38.05/67.26	8	32	2.00E-03	3
304	Peptidyl-prolyl cis-trans isomerase-A	P62937	7.68/8.09	18.23/27.67	11	61	4.30E-46	1
305	FK506-binding protein-1A	P62942	7.88/8.05	12.00/20.77	6	50	6.80E-12	1
306	Ubiquitin	P62988	6.56/6.97	8.56/23.81	6	61	2.30E-24	3
307	Growth factor receptor-bound protein-2	P62993	5.89/6.2	25.30/47.79	15	61	9.20E-32	2
308	14-3-3 protein-ζ/δ	P63104	4.73/5.31	27.90/53.92	14	56	2.30E-42	3
309*	Eukaryotic translation initiation factor-5A-1	P63241	5.08/5.63	17.05/29.02	6	45	6.00E-04	3
310*	Guanine nucleotide-binding protein subunit-β-2-like 1	P63244	7.56/7.56	35.51/63.97	18	70	4.30E-33	3
311	Actin, cytoplasmic-2	P63261	5.31/5.80	42.11/76.93	17	46	3.60E-57	1
312	Ser/Thr protein phosphatase-2A catalytic subunit-α-isoform	P67775	5.30/5.76	36.14/70.58	10	45	3.30E-06	3
313*	Elongation factor-1-α-1	P68104	9.10/7.87	50.45/106.51	7	19	1.50E-19	6
314*	Tubulin-α-ubiquitous chain	P68363	4.94/5.99	50.80/87.80	13	39	4.60E-07	2
315*	Tubulin-β-2C chain	P68371	4.79/5.59	50.26/95.91	18	38	1.50E-29	3
316*	Histone-H3.1	P68431	11.27/8.58	15.44/27.15	4	20	2.70E-07	3
317	Hemoglobin subunit-β	P68871	6.75/7.05	16.10/19.88	13	89	4.30E-79	1
318	Hemoglobin subunit-α	P69905	8.72/8.49	15.31/233.09	6	62	2.70E-34	1
319*	T-complex protein-1-subunit-β	P78371	6.01	57.79	14	42	6.29E-10	6
320*	Glutathione transferase-ω-1	P78417	6.23/6.36	27.83/52.67	16	46	7.30E-35	1
321	Neutrophil gelatinase-associated lipocalin precursor	P80188	9.02/8.04	22.74/41.77	12	63	1.20E-17	4
322	Protein S100-A12	P80511	5.83/6.30	10.57/11.87	6	45	1.70E-21	1
323*	Nuclear protein Hcc-1	P82979	6.13/6.46	23.71/59.89	4	18	2.30E-03	3
324*	ADP-ribosylation factor 1	P84077	6.32/6.31	20.70/29.64	11	69	8.50E-16	3
325	Histone-H3.3	P84243	11.27/7.29	15.38/26.42	8	44	2.10E-14	3
326*	Sorbitol dehydrogenase	O00796	8.25/9.59	38.90/63.57	12	36	2.80E-05	6
327	Adenylyl cyclase-associated protein-1	O01518	8.12/6.70	52.22/109.94	8	27	6.80E-17	6
328*	Lactoylglutathione lyase	O04760	5.12/5.38	20.99/35.44	6	32	1.00E-03	1
329	Galectin-10	O05315	6.82/7.15	16.58/20.60	6	66	1.10E-11	1
330	Proteasome activator complex subunit-1	O06323	5.78/6.14	28.88/59.02	15	61	1.80E-30	3
331*	Peroxiredoxin-1	O06830	8.27/8.26	22.32/40.87	18	75	2.30E-64	1
332*	Splicing factor, arginine/serine-rich-1	O07955	10.37/6.40	27.84/68.78	9	38	4.80E-05	3
333	Rho-GTPase-activating protein-1	O07960	5.85/6.34	50.46/96.08	21	57	1.80E-25	3
334*	Secernin-1	O12765	4.66/5.14	46.80/10.21	12	29	9.20E-07	3
335*	Nuclear pore complex protein Nup160	O12769*	5.41/9.17	151.13/83.21	12	12	4.60E-03	3
336*	δ-(3,5)-δ-(2,4)-Dienoyl-CoA isomerase	O13011	8.16	36.14	7	25	2.51E-06	6
337*	Ubiquitin-conjugating enzyme E2 variant-1	O13404	8.56/6.07	26.07/55.70	8	32	4.60E-07	4

Table 1. Continued

ID no. ^{a)}	Protein name	SwissProt Access. no. ^{b)}	Theoret./observ. p/ ^{c)}	Theoret./observ. Mr ^{d)} (kDa)	Pept. match. (n)	Seq. cov. ^{e)} (%)	Mascot expect. score ^{f)}	Sub. cell. fract. no. ^{g)}
338*	Dynactin subunit-2	Q13561	5.10/5.30	44.19/52.24	10	35	1.70E-06	6
339*	NEDD8-activating enzyme E1 subunit	Q13564	ND	ND	ND	ND	1.20E-04	6
340*	Spectrin- α -chain, brain	Q13813	5.22/5.55	285.16/203.12	40	23	7.30E-18	2
341*	Spliceosome RNA helicase BAT1	Q13838	5.44/5.99	49.42/95.04	15	35	9.20E-18	3
342*	Coactosin-like protein	Q14019	5.54/6.69	16.05/25.85	12	57	3.40E-19	4
343	Heterogeneous nuclear ribonucleoprotein D0	Q14103	7.62/5.93	38.58/91.86	7	22	5.20E-05	4
344*	Septin-6	Q14141	6.24	50.08	17	35	7.92E-08	6
345*	Keratin, type I cuticular Ha3-II	Q14525	4.81/5.77	47.33/192.32	14	44	1.50E-12	2
346*	Neutral- α -glucosidase AB precursor	Q14697	5.74/6.21	107.26/196.40	24	28	9.20E-13	3
347*	Major vault protein	Q14764	5.34/5.86	99.55/174.43	19	22	1.70E-11	2
348	LIM and SH3 domain protein-1	Q14847	6.61/6.81	30.10/71.22	10	33	1.80E-11	3
349*	Orphan nuclear receptor NR1I3	Q14994	ND	ND	ND	ND	2.50E-03	6
350*	Septin-2	Q15019	6.15/6.48	41.69/72.94	7	26	1.60E-04	2
351	Neutrophil cytosol factor-4	Q15080	6.40/6.49	39.12/74.10	8	26	1.80E-11	2
352*	Protein disulfide-isomerase A6 precursor	Q15084	4.95/5.42	48.90/88.78	15	43	2.90E-15	3
353*	Poly(rC)-binding protein-1	Q15365	6.66	37.99	7	30	3.97E-08	6
354	Ras suppressor protein-1	Q15404	8.57/8.54	31.52	16	56	1.10E-27	3
355*	Protein phosphatase-1-regulatory subunit-7	Q15435	4.84/5.39	41.65	10	32	3.90E-06	3
356*	Syntaxin-binding protein-2	Q15833	6.11/6.45	66.85	13	33	1.80E-09	3
357*	Ras-related protein Rab-11B	Q15907	5.65/5.80	24.59	9	40	2.70E-24	3
358*	Histone H2A type 2-C	Q16777	10.90/6.70	14.00/26.34	4	49	7.80E-04	3
359*	Short chain 3-hydroxyacyl-CoA dehydrogenase, mitochondrial precursor	Q16836	8.88/5.86	34.21/27.24	10	38	1.80E-18	4
360	Thioredoxin reductase-1, cytoplasmic precursor	Q16881	6.07	55.47	11	27	1.58E-08	6
361*	Chaperonin containing TCP1, subunit 8	Q53HU0	ND	ND	ND	ND	1.40E-05	6
362	This TrEMBL entry deleted	Q5JV65	ND	ND	ND	ND	4.80E-26	6
363*	Histone-H2B type 2-F	Q5QNW6	10.31/9.82	13.98/27.27	8	61	5.80E-20	3
364*	Twinfilin-2	Q6BS0	6.37/6.71	39.75/79.74	10	42	4.60E-07	3
365*	NAPRT Protein	Q6PJ1	ND	ND	ND	ND	5.50E-24	6
366*	Staphylococcal nuclease domain-containing protein-1	Q7KZF4	6.74/6.92	102.62/200.89	21	27	7.30E-14	3
367*	Histone-H2A type 3	Q770	11.05/5.96	14.10/25.95	5	35	8.50E-21	3
368*	Keratin, type II cytoskeletal-1b	Q7Z794	ND	ND	ND	ND	3.00E-11	6
369*	Unc-112-related protein-2	Q86UX7	6.52/6.21	76.48/68.65	23	29	4.60E-22	3
370*	Ras-related protein Rab-43	Q86YS6	5.44/5.10	23.55/56.43	7	45	5.80E-07	4
371*	Dedicator of cytokinesis protein-3	Q8ZD9	6.52/9.18	235.01/33.43	12	7	8.00E-03	6
372*	Nesprin-1	Q8N9F1	5.38	1011.04	35	6	3.15E-03	6
373*	γ -Glutamyl hydrolase precursor	Q92820	6.67/6.59	36.34/59.02	4	14	4.30E-04	1
374*	Probable ATP-dependent RNA helicase DDX17	Q92841	8.82/9.65	72.95/105.93	13	22	8.20E-03	6
375*	Histone-H2A type 1-C	Q93077	11.05/3.49	14.10/18.34	5	23	6.80E-10	3
376*	Histone-H2B type 1-H	Q93079	10.31/8.86	13.93/27.11	3	27	5.40E-10	3
377*	Uncharacterized protein C19orf10 precursor	Q960H8	6.20/6.16	18.90/53.14	4	27	2.20E-03	4
378*	Far upstream element-binding protein-1	Q96AE4	7.18/8.36	67.69/60.93	19	39	2.90E-33	4
379*	EF-hand domain-containing protein-2	Q96C19	5.15/5.37	26.79/57.61	23	62	3.60E-28	2

Table 1. Continued

ID no. ^{a)}	Protein name	SwissProt Access. no. ^{b)}	Theoret./observ. p/ ^{c)}	Theoret./observ. (kDa)	Pept. match. (n)	Seq. cov. ^{e)} (%)	Mascot expect. score ^{f)}	Sub. cell. fract. no. ^{g)}
380*	Phosphoglucosyltransferase-2	O96G03	6.28	68.75	19	35	1.26E-09	6
381*	ERO1-like protein- α -precursor	O96HE7	5.48/5.87	55.21/127.76	11	27	2.90E-11	3
382*	Abhydrolase domain-containing protein-14B	O96IU4	5.94/6.05	22.45/36.45	6	38	2.10E-03	1
383*	Histone H2A type 1-H	O96KK5	10.88/7.06	13.93/20.48	5	38	2.70E-08	3
384	Cytosolic nonspecific dipeptidase	O96KP4	5.66	53.19	12	35	6.29E-04	6
385	RNA-binding protein-14	O96PK6	9.68/9.71	69.62/102.34	14	25	8.50E-04	6
386	Calponin-2	O99439	6.92/6.99	34.07/60.59	14	49	1.10E-11	2
387*	Synaptic vesicle membrane protein VAT-1-homolog	O99536	5.88/6.17	42.12/82.48	16	50	4.60E-14	3
388*	Translin-associated protein-X	O99598	6.10/6.38	33.21/60.00	10	50	1.50E-06	2
389*	Monoglyceride lipase	O99685	6.49/6.18	33.47/67.37	6	24	7.40E-04	4
390*	3-Hydroxyacyl-CoA dehydrogenase type-2	O99714	7.66/6.25	27.13/18.90	7	11	3.60E-04	4
391*	Aconitate hydratase, mitochondrial precursor	O99798	7.36/6.76	86.11/52.51	13	20	9.20E-42	4
392*	Copine-1	O99829	5.52/5.92	59.65/119.95	13	24	2.30E-22	1
393	Histone-H2A type 1-J	O99878	10.88/5.71	13.93/25.78	6	38	1.10E-15	3
394*	Uncharacterized protein C9orf142	O9BUH6	5.39/5.60	21.97/38.08	9	42	3.40E-09	2
395*	Transmembrane emp24 domain-containing protein-9-precursor	O9BVK6	6.67/6.57	25.20/40.69	11	55	2.70E-06	2
396*	Kinesin light chain-2	O9H0B6	6.72/6.36	69.29/79.92	14	29	8.20E-03	2
397*	Haloacid dehalogenase-like hydrolase domain-containing protein-2	O9H0R4	ND	ND	ND	ND	1.70E-05	6
398*	Ras-related protein Rab-1B	O9H0U4	5.55/5.64	22.33/41.56	4	20	2.10E-05	3
399	EH domain-containing protein-1	O9H4M9	6.35	60.65	13	26	9.98E-04	6
400*	Sideroflexin-1	O9H9B4	9.22/5.90	35.88/27.94	10	34	1.30E-05	4
401*	Phosphopantothenate--cysteine ligase	O9HAB8	6.25/6.74	33.98/65.20	8	24	2.00E-06	3
402	Retinoid-inducible serine carboxypeptidase precursor	O9HB40	5.61/6.34	51.08/26.26	8	15	4.60E-08	1
403*	Adipocyte plasma membrane-associated protein	O9HDC9	5.82/7.04	46.62/50.00	21	48	2.90E-38	4
404*	Exosome complex exonuclease RRP41	O9NPD3	6.08/6.39	26.65/48.50	9	40	6.60E-04	2
405	Protein FAM49B	O9NUC9	5.76/6.03	37.01/60.98	16	49	4.60E-22	1
406	Dipeptidyl-peptidase-3	O9NY33	5.02/5.37	82.88/153.84	9	12	9.20E-18	3
407*	Tropomodulin-3	O9NY 9	ND	ND	ND	ND	1.20E-29	6
408*	EH-domain-containing protein-3	O9NZN3	6.06/6.44	61.97/50.21	12	24	7.60E-04	2
409*	Vacuolar protein sorting-29	O9UBQ0	6.29/6.70	20.66/35.44	8	43	3.60E-13	2
410	Fructose-1,6-bisphosphate aldolase A [Fragment]	O9UCN2	ND	ND	ND	ND	7.20E-05	6
411*	Protein NipSnap3A	O9UFN0	9.21/8.65	28.56/37.28	6	25	5.20E-06	6
412*	Mitogen-activated protein kinase kinase-1	O9UHA4	13.67/6.59	13.67/24.23	3	43	3.60E-07	3
413*	N-acetylglucosamine kinase	O9UJ70	5.82/6.11	37.69/70.84	14	44	5.40E-15	2
414*	DCC-interacting protein-13- α	O9UKG1	ND	ND	ND	ND	6.90E-08	6
415*	Proteasome activator complex subunit-2	O9U 46	5.44/5.69	27.52/55.19	11	43	5.20E-06	2
416*	Apoptosis-associated speck-like protein containing a CARD	O9U Z3	5.95/6.54	21.67/38.14	7	37	7.30E-09	1
417	Protein-arginine deiminase type-4	O9UM07	6.15/6.58	75.13/116.76	9	19	4.60E-08	2
418*	NSFL1 cofactor-p47	O9UNZ2	ND	ND	ND	ND	5.50E-17	6
419*	RuvB-like 2	O9Y230	5.49/5.73	51.30/87.80	18	43	5.40E-11	2

Table 1. Continued

ID no. ^{a)}	Protein name	SwissProt Access. no. ^{b)}	Theoret./observ. p/ ^{c)}	Theoret./observ. Mr ^{d)} (kDa)	Pept. match. (n)	Seq. cov. ^{e)} (%)	Mascot expect. score ^{f)}	Sub. cell. fract. no. ^{g)}
420*	Cofilin-2	O9Y281	7.66/7.49	18.84/29.00	5	28	1.50E-03	1
421*	Trafficking protein particle complex subunit-4	O9Y296	5.83/6.24	24.44/40.69	13	60	3.60E-14	2
422*	SH3 domain-binding protein-1	O9Y33	6.33/6.44	76.01/139.19	4	5	1.00E-03	2
423*	Talin-1	O9Y490	5.77/6.23	271.77/231.63	47	27	2.90E-45	1
424	Heme-binding protein-2	O9Y524	4.58/5.81	22.86/69.71	3	18	4.60E-12	3
425*	Actin, α -cardiac muscle-1	P68032	5.23	42.33	4	16	1.58E-03	6
426*	High mobility group protein-B2	P26583	5.62/7.16	24.92/44.58	11	43	5.80E-28	4

a) Asterisk indicates proteins not previously identified in EOSs.

b) SwissProt accession number.

c) Theoretical/observed p/.

d) Theoretical/observed Mr.

e) Percent peptides analyzed.

f) Mascot expectation score.

g) Subcellular fraction. (1) cytoplasm, (2) cytoskeleton, (3) nucleus, (4) organelle, (5) Zoom IEF, (6) whole cell lysate.

h) ND = Not determined.

principally proved valuable in reducing protein complexity and increasing low abundance proteins. Figure 4 is a Western blot analysis that shows the distribution of eight randomly selected proteins into the four subcellular fractions (F1–F4) demonstrating in part the effectiveness of the differential fractionation method.

Actin was the most prominent protein expressed in EOSs. Because of this fact, we chose to comparatively evaluate actin levels in other leukocytes. Figure 5 shows the comparative distribution of actin and an actin proteolytic cleavage fragment by Western blot analysis of monocyte, neutrophil, and EOS cell lysates.

3.2 Ingenuity Pathway Analysis software application

Ingenuity software was applied to the analysis of the EOS expression data set to probe the relevant biological functions of the identified proteins in the data set (Table 1). Some functions and diseases relevant to the data set are shown in Fig. 6. Figure 7 shows selected groups of proteins that highlight in more detail the proportion of the identified proteins whose function or impact are particularly relevant to EOS biological activity; namely, immunological disease, inflammatory disease, immune response, immune and lymphatic system development and function, and respiratory disease. Figure 8 gives a histogram of the top canonical pathways associated with the data set. A small *p*-value indicated a strong association between the data set and the respective pathway. Proteins found in selected EOS disease functional and canonical pathway subsets (Figs. 6 and 8) are listed in Supporting Information Tables S1 and S2 (see www.proteomics-journal.com).

4 Discussion

We have identified 3141 proteins, which had Mascot expectation scores of 10^{-3} or less. Of these, 426 proteins were unique and non-redundant as identified using the SwissProt protein database. We did not attempt to distinguish differences between males and females nor did we address the extent of observed polymorphic variations between individuals since large numbers of donors would be required. However, further studies are planned to deal with these important issues. Significantly, of the 426 non-redundant proteins 231 were novel proteins not previously reported to occur in EOSs. Since only 8% of all proteins excised and analyzed from 2-D gels were among the unique, non-redundant data set (426 proteins), the question arises as to the occurrence and nature of the redundant protein data set (2715 proteins).

There are many explanations for protein redundancy including phosphorylation. We undertook a preliminary assessment of the EOS phosphoproteome using Pro-Q

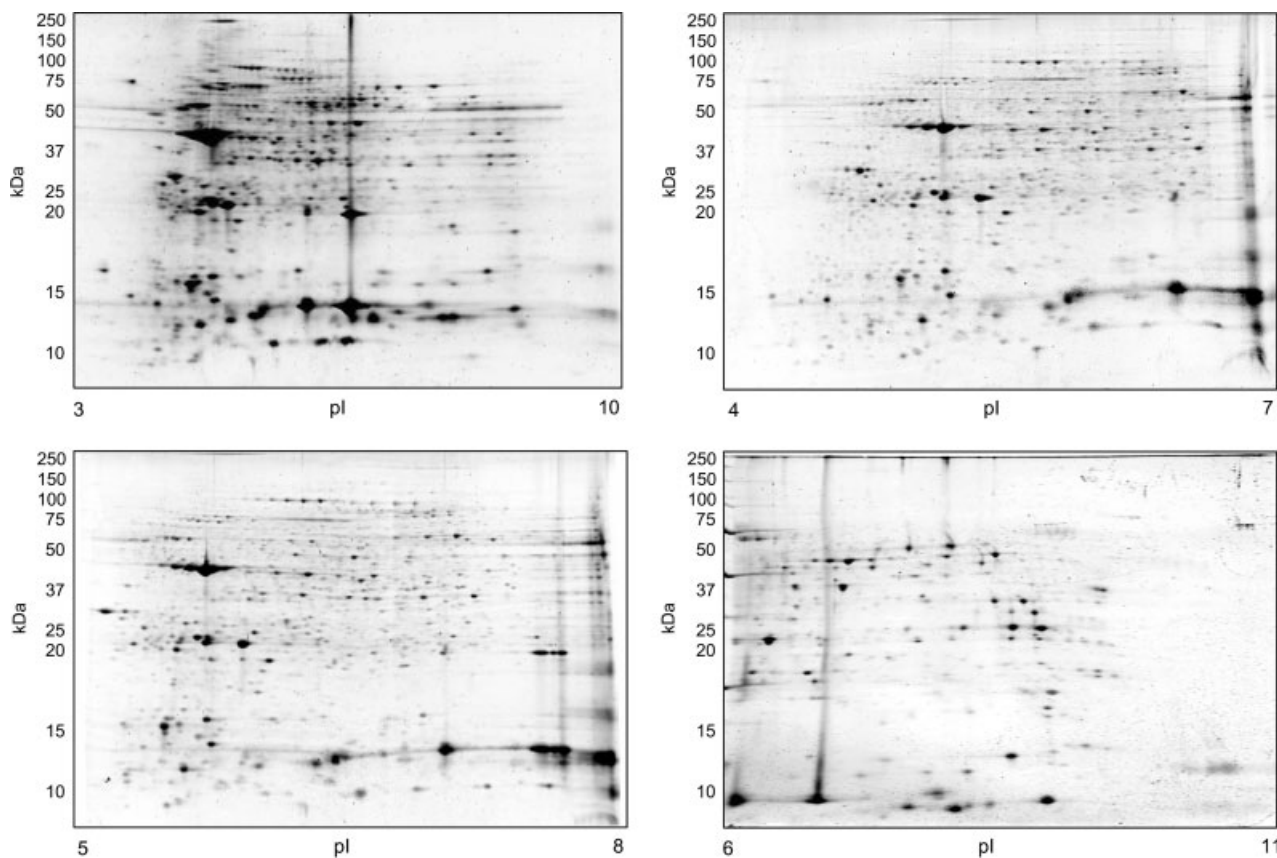


Figure 2. Comparison of EOS proteome maps focused at four different pH ranges: 3–10; 4–7; 5–8; and 6–11. Each gel was loaded with 200 µg of total EOS cell lysate.

Diamond staining in order to evaluate the contribution of phosphorylation to redundancy (results not shown). The characterization of the EOS phosphoproteome by 2-DE will be separately reported. We found that many EOS proteins were phosphorylated; phosphorylation can be variable at a given site and may be variable as to the number of sites modified all of which contribute to redundancy. In addition, as shown in Fig. 1, 2-D gel analysis indicated a number of horizontal protein spots, identified as the same protein by MS, with the same Mr, but having different pIs, indicating polymorphism and/or posttranslational modification. In addition to phosphorylation, a number of modifications can account for such variations; as for example, acetylation, sialylation, sulfation, and methylation. Furthermore, since many proteins have attached carbohydrate moieties, these can give rise to significant pI and/or Mr variations. Finally, proteolytic processing/modifications must be considered among the relevant causes of protein redundancy. Clearly, the above examples are not an exhaustive list of factors leading to protein redundancies. The observed high protein redundancy likely reflected the dynamic character of the EOS and underscores the fact that posttranslational modifications may be the result of various regulatory and signaling events.

This proteomic data set is the largest comprehensive proteomic data set of proteins expressed in normal peripheral blood EOSs reported to date. There have been two reports of comparative proteomic studies. Waschnagg *et al.* [12] very recently evaluated protein expression differences induced by Birch pollen allergy and identified 97 unique non-redundant EOS proteins of which 90 occur in our list of 426 (Table 1), which is an excellent agreement. However, a comparative proteomic study of healthy *versus* atopic dermatitis patients identified 51 differentially expressed proteins of which only three are included in Table 1 [13].

In this study, we have made some attempt at characterizing the less abundant proteins using ZOOM[®] pre-fractionation IEF and subcellular fractionation methods. Protein distribution into various fractions using a commercial subcellular fractionation method allowed for the reduction of protein complexity and increased the number of less abundant proteins observed. We found that this fractionation method performed better in reducing protein losses than many other subcellular fractionation methods that can incur appreciable protein loss. Furthermore, the differential solubilization method was amenable to small sample size, gave high protein recoveries, had relatively high throughput, and processing time was fairly short minimizing protein

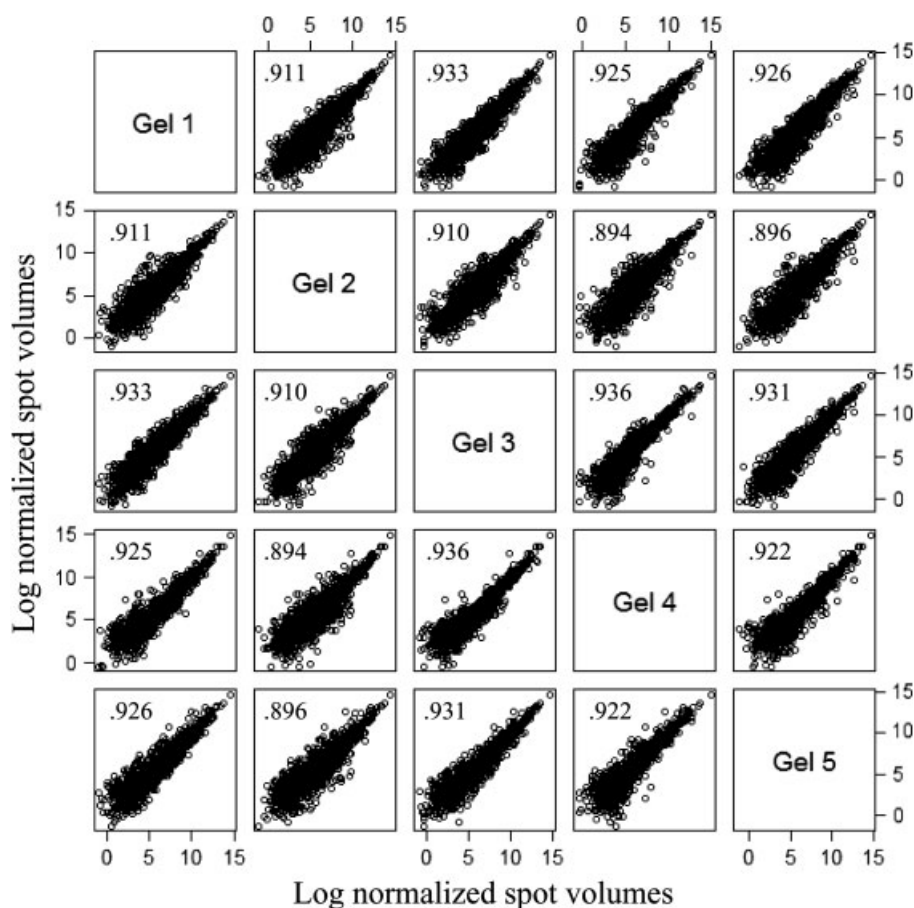


Figure 3. Gel-to-gel correlation of five replicate gels showing 2-DE reproducibility. Log normalized spot volumes for gel 1 were plotted pairwise versus gels 2–5 and the Pearson's correlation coefficient shown in squares was calculated. Gels (11 cm) were focused over the pH range 3–10 and were stained with Sypro Ruby. Gel image analysis utilized Nonlinear SameSpots software.

Table 2. Summary prefractionation protein ID's

Fractions analyzed	Protein IDs	Non-redundant Protein IDs ^{a)}
Subcellular fractions^{b)}		
1-Cytoplasm	625	95
2-Organelle	425	50
3-Nucleus	693	141
4-Cytoskeleton	345	52
Total subcellular	2088	338
IEF fractions^{c)}		
pH 3.0–5.4	44	4
pH 5.4–7.0	181	13
pH 7.0–10.0	226	16
Total IEF	451	33
Whole cell lysate	480	63
Total all fractions	3019	434

a) Had Mascot expectation scores of 10^{-3} or less.

b) According to Calbiochem's ProteoExtract[®] Subcellular Proteome Extraction kit.

c) Using ZOOM[®] IEF Fractionator (Invitrogen).

alterations. However, this method is not sufficiently adequate to predict protein localization to specific subcellular compartments.

Characterization of the data set (Table 1) using Ingenuity Pathway Analysis (IPA) revealed a number of interesting features. Especially, worthy of note was that 312 of the 434 (72%) identified non-redundant proteins could be subdivided into categories (Fig. 6) which were related to known EOS biological activities directly; e.g. eosinophilia, cell movement, chemotaxis, and activation, or indirectly; e.g. autoimmune diseases. We were able to detect and positively identify many proteins that were relevant to EOS functions involving survival and activation. Recent studies strongly suggest that tissue eosinophilia is more dependent on increased survival in peripheral tissues than increased *de novo* generation in the bone marrow followed by blood to tissue translocation [14]. Analysis of EOS turnover *in vivo* revealed their active recruitment to the peritoneal cavity and their prolonged survival there [14]. In this regard, our IPA showed a considerable number of proteins (~125) involved in cell death and survival (Fig. 6). Most of these proteins have previously not been correlated with EOS survival processes. However, some of these proteins were shown to play roles in other aspects of EOS biology. These observations emphasized the need for more studies to investigate the pro- and anti-apoptotic proteins that regulate EOS survival in end organs to induce or prevent apoptosis in cells

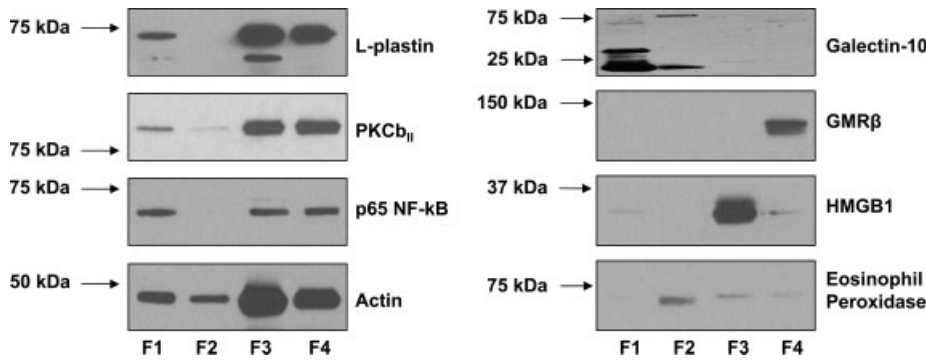


Figure 4. Western blot analysis of eight randomly selected EOS proteins to demonstrate their distribution by differential solubility using a commercial kit (Calbiochem's ProteoExtract® Subcellular Proteome Extraction kit). The kit employed four solubility fractions F1–F4 as shown (see also Table 2). A total of 50 µg cell lysates were applied to each lane.

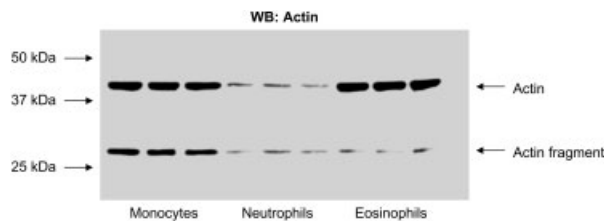


Figure 5. Western blot analysis comparing actin levels in monocytes, neutrophils, and EOSs in triplicate. A total of 50 µg cell lysate protein was loaded in each lane. Actin fragment was an N-terminal product as a result of proteolysis (see Section 4).

depending on whether the need is to protect against helminth parasites or ameliorate EOS-associated diseases.

EOSs are secretory cells that contain large amounts of granules occupying about one-fifth of the cytoplasm [1]. Four major populations of granules have been identified; namely, primary, secondary, small granules, and as well lipid bodies [1]. Our 2-DE studies identified four of the major proteins found in the secondary granules that included, ECP, EDN, EPO, and MBP as well as galectin-10 found in the primary granules. Numerous other proteins have also been reported to occur in the granules [1]. ECP is a secretory ribonuclease associated with host defense against non-phagocytosable pathogens, such as helminthic parasites. It also has antibacterial activity, which is not shared by EDN, another closely related neurotoxic EOS ribonuclease. The mechanism

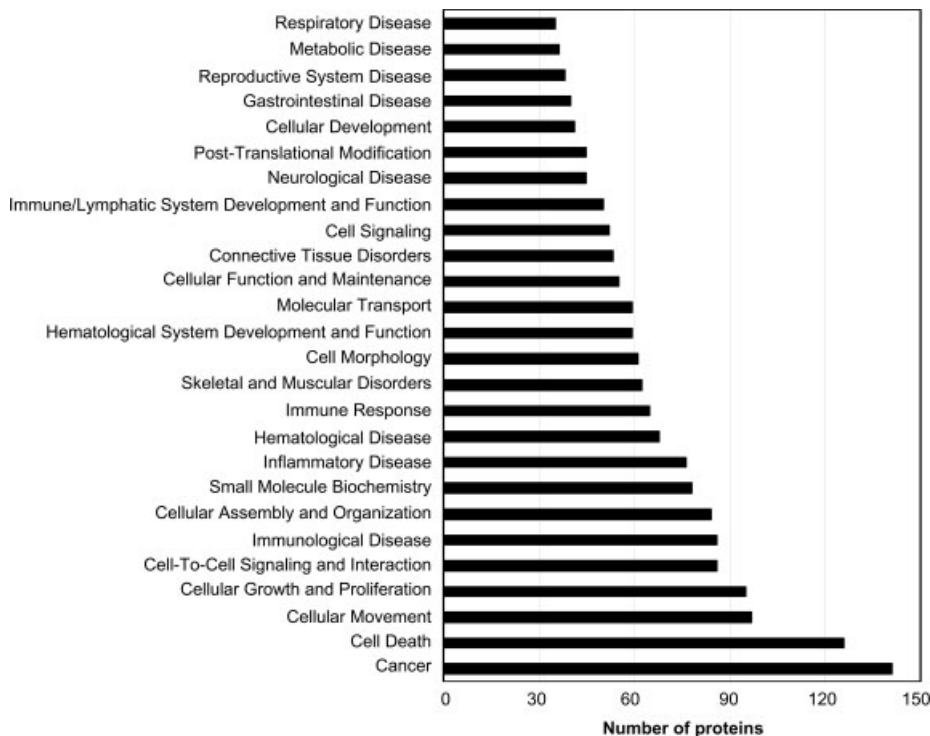


Figure 6. IPA showing the distribution of identified EOS proteins from Table 1 into disease and functional categories.

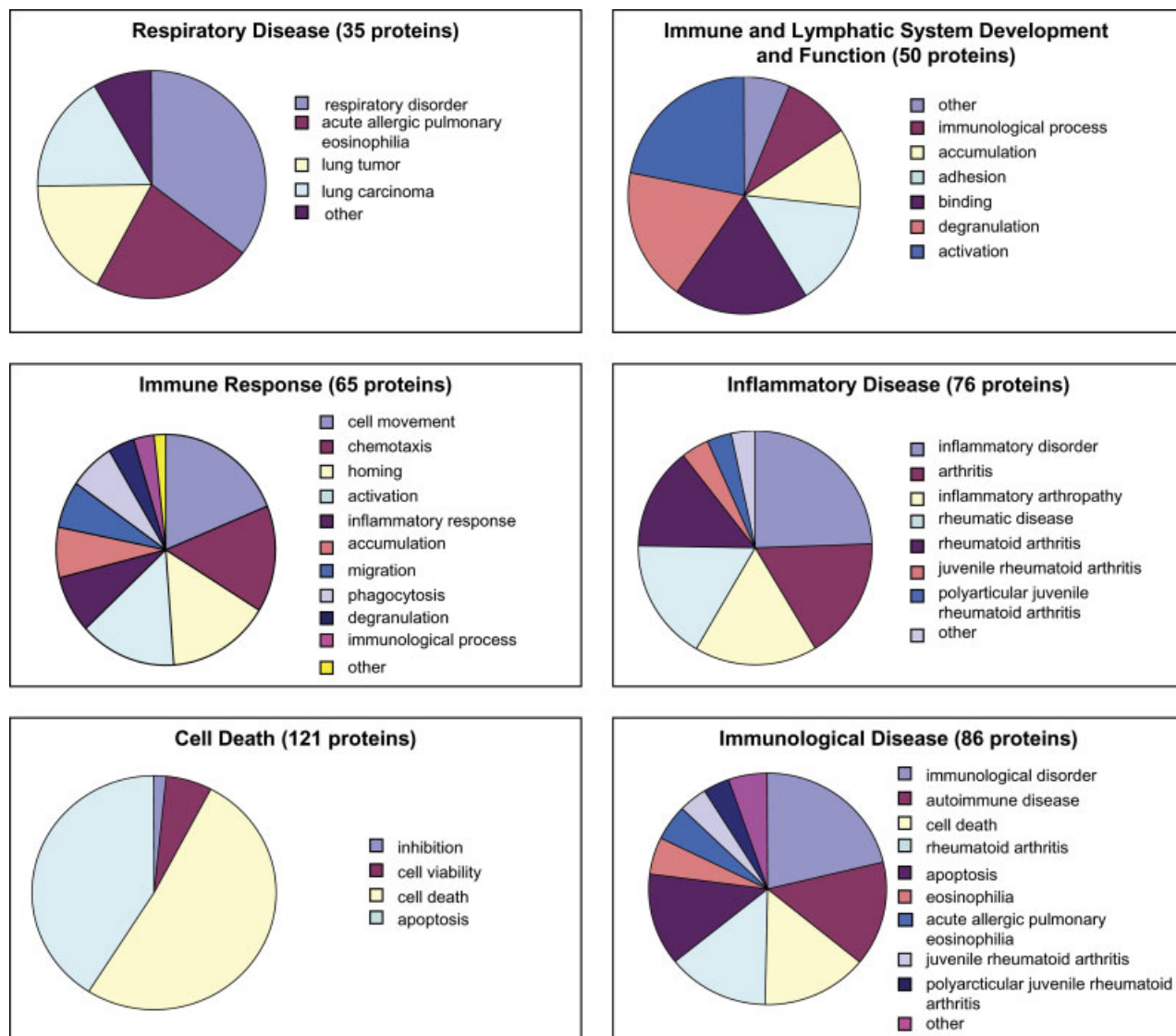


Figure 7. Subclassification of eosinophilic proteins from Table 1 and Fig. 6 shows a distribution of eosinophilic proteins into diseases and functional categories highly consistent with what is general appreciated regarding eosinophilic biological activity.

of action of ECP is thought to involve pore formation in target membranes, which is apparently not dependent on its RNase activity [15]. On the other hand, EDN, which shares 70% homology with ECP has been implicated in antiviral activity against respiratory infections mainly due to its ribonuclease activity [16]. EPO is an EOS haloperoxidase that catalyzes the peroxidative oxidation of halides present in the plasma as well as hydrogen peroxide generated by dismutation of superoxide produced during respiratory burst. This reaction leads to the formation of bactericidal hypohalous acids [17]. MBP was traditionally associated with toxicity against helminthic worms and is at least partly responsible for tissue damage in bronchial mucosa in asthma. The mechanism of its action is believed to be increased membrane permeability through surface charge interactions

leading to perturbation of the cell-surface lipid bi-layer. These granule proteins are actively released from activated EOSs and little if any active transcription occurs in mature EOSs. The role of EOSs in the pathophysiology of bacterial and viral infections is still not well elucidated.

The second most abundant and notable protein observed by 2-D gel analysis of EOS cell lysates was galectin-10 (Table 1, Fig. 1; ID 329), which occurs mainly in the primary granules of EOSs and for many years was referred to as lysophospholipase or Charcot-Layden crystal protein. However, new evidence gives strong indication that it belongs to the galectin superfamily of proteins and was designated as galectin-10 by Ackerman *et al.* [18, 19]. Previously galectin-10 was thought to occur only in EOSs and basophils, but recent work has also identified it in

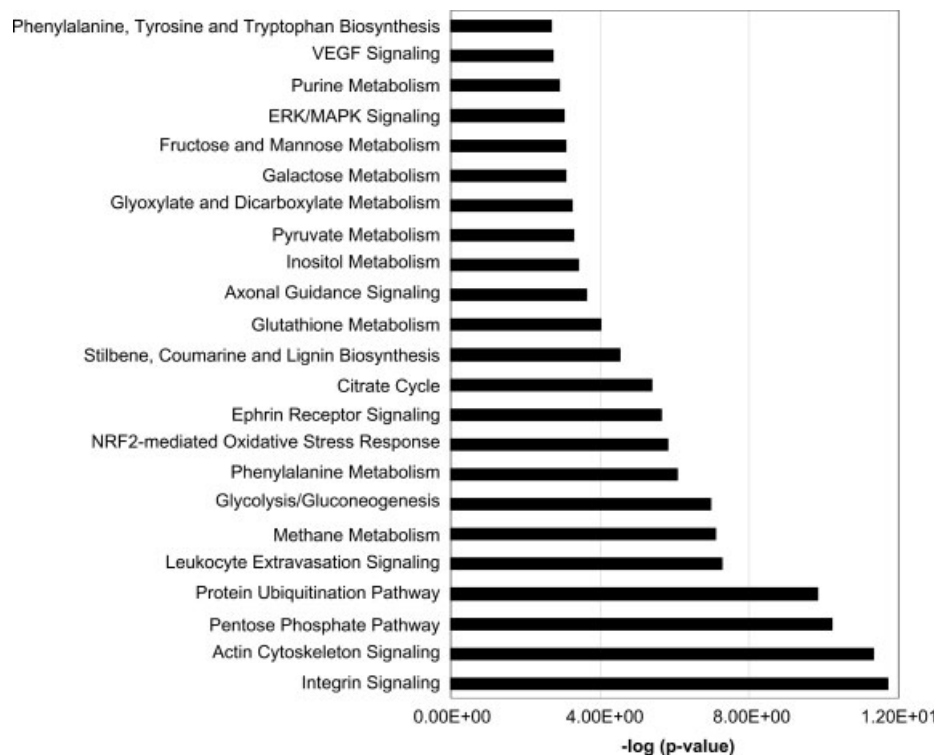


Figure 8. IPA showing the distribution of identified EOS proteins (Table 1) into canonical pathways showing a strong emphasis on signaling pathways consistent with the dynamic nature of the EOS.

human CD4⁺CD25⁺ regulatory T cells (CD25⁺ Treg cells) where it is thought to function in maintaining immunological self-tolerance by suppressing autoaggressive T cells [20]. Eosinophilic galectin-10 also appears to have lectin-like properties and can bind mannose (in the crystal) [18]. Further investigations are required to elucidate the biological function of this interesting protein. Gel analysis results from both 1-D and 2-D gels, including Western blot analysis using anti-galectin-10, showed that galectin-10 distributed in multiple gel locations. Repeated gel analysis by 1-D SDS-PAGE and Western blotting of EOS cell lysates gave three bands of molecular weights ~17, ~25, and ~75 kDa. Galectin-10 has been reported to be unique in having a propensity to aggregate even in dissociating conditions [21]. Gel analysis by 2-DE was also anomalous with spots at ~17 and ~25 kDa and pronounced vertical streaking likely due to precipitation at its *pI* in the first dimension of 2-DE (Fig. 1). Some dimer formation was also noted (Fig. 1). Western blot 2-DE analysis of galectin-10 also showed multiple horizontal spots at ~17 kDa indicating polymorphism and/or posttranslational modifications. *N*-terminal acetylation and isoforms for galectin-10 were also identified by 2-DE of CD25⁺ Treg-cell lysates and human EOSs [20]. A separate study will be required to fully characterize the various isoforms associated with galectin-10.

The 2-D gels showed that EOSs have especially high amounts of actin (Fig. 1, Table 1; ID 311), which contributed to the relatively lower abundance of other proteins in the cell lysate samples. Actin cytoskeletal structures and associated proteins likely play important roles in EOS

functions, such as signaling (Fig. 8), cell motility, degradation, phagocytosis, and activation [22–24]. Some of the actin was proteolytically processed to smaller Mr forms (Figs. 1 and 5; Table 1; ID 275) and some actin was also phosphorylated (Pro-Q Diamond staining not shown). Actin phosphorylation in other cells was previously reported [25, 26] and plays an important role in actin polymerization [27, 28]. Protein MS ID did not distinguish between β - or α -actin since β - and α -actin have virtually identical primary structures. Although non-muscle actin and actin-associated proteins are reported to occur in the nucleus of cells [29], our previous studies using FITC-phalloidin, anti- α -fodrin [24], and anti-actin (results not shown) did not indicate the occurrence of nuclear actin in EOSs. However, these results could not rule out the occurrence of very low levels of nuclear actin that could not be detected under the experimental conditions employed or that the actin Ab was not reactive to nuclear actin due to some unique complex formation. Actin levels in EOSs and monocytes were relatively high when compared with neutrophils with considerably more proteolytic processing occurring in monocytes (Fig. 5). This was also confirmed by 2-DE of cell lysates (results not shown). The observed actin fragment represented the *N*-terminal domain of actin, since the anti-actin antibody used was raised against an *N*-terminal fragment (actin 1–19). Numerous actin complex-associated proteins were identified; for example, actin-related protein 2/3 complex, gelsolin, vimentin, Rho GDP-dissociation inhibitor, transgelin, moesin, coactosin-like protein, tubulin, cofilin, γ -plastin, calreticulin, myosin, F-actin capping

proteins cap Z α -1 and β , and macrophage protein G, α -actinin, profilin, dynactin, coronin, nesprin, kinesin, tropomodulin, talin, and spectrin. The facile ID of these proteins was undoubtedly related to the high level expression of cytoplasmic actin in EOSs. The high actin level and abundant associated proteins underscore the importance of the cytoskeleton in the biological activity of EOSs especially motility and activation

An important advantage of proteomic analysis by 2-DE is the visualization and potential ID of polymorphisms and/or post-translational modifications. Figure 1 shows a number of proteins that are likely to be posttranslationally modified as evidenced by repeated horizontal protein spots from the same protein identified by MS; for example, Fig. 1, Table 1; ID's 31, 36, 45, 48, 49, 50, 53, 59, 61, 66, 107, 135, 167, 182, 193, 216, 257, 283, 304, and 329. Some of these proteins have not been previously reported to be posttranslationally modified; as for example, Table 1: 31, 59, 107, 135, and 257.

In summary, the herein described protein expression results represent the largest comprehensive reporting of the human EOS proteome. The ID of proteins in any proteome study is somewhat asymptotic and probably not 100% achievable by current technologies. This proteome map will be especially valuable as a baseline to compare with EOSs from disease and pharmacologically treated states.

This study was supported by the National Institutes of Health, National Heart, Lung and Blood Institute's Proteomics Initiative NO1-HV-28184 (to A. K.), the National Institutes of Health grants 1-R24 CA88317 (to A.K.), 1-P30 ES06676 (to C. Elferink) and 1-P01AI062885 (to A. Brasier).

The authors have declared no conflict of interest.

5 References

- [1] Giembycz, M. A., Lindsay, M. A., Pharmacology of the eosinophil. *Pharmacol. Rev.* 1999, 51, 213–339.
- [2] Rothenberg, M. E., Hogan, S. P., The eosinophil. *Annu. Rev. Immunol.* 2006, 24, 147–174.
- [3] Ganley-Leal, L. M., Mwinzi, P. N., Cetre-Sossah, C. B., Andove, J. *et al.*, Correlation between eosinophils and protection against reinfection with *Schistosoma mansoni* and the effect of human immunodeficiency virus type 1 coinfection in humans. *Infect. Immun.* 2006, 74, 2169–2176.
- [4] Melo, R. C. N., Spencer, L. A., Dvorak, A. M., Weller, P. F., Mechanisms of eosinophil secretion: large vesiculotubular carriers mediate transport and release of granule-derived cytokines and other proteins. *J. Leukoc. Biol.* 2008, 83, 229–236.
- [5] Pazdrak, K., Young, T. W., Stafford, S., Olszewska-Pazdrak, B., Straub, C. *et al.*, Cross-Talk between ICAM-1 and granulocyte-macrophage colony-stimulating factor receptor signaling modulates eosinophil survival and activation. *J. Immunol.* 2008, 180, 4182–4190.
- [6] Cramer, R., Dri, P., Zabucchi, G., Patriarca, P., A simple and rapid method for isolation of eosinophilic granulocytes from human blood. *J. Leukoc. Biol.* 1992, 52, 331–336.
- [7] Wardlaw, A., Eosinophil density: what does it mean? *Clin. Exper. Allergy* 1995, 25, 1145–1149.
- [8] Gruart, V., Balloul, J. M., Prin, L., Tomassini, M., Variations in protein expression related to human eosinophil heterogeneity. *J. Immunol.* 1989, 142, 4416–4421.
- [9] Fukuda, T., Gleich, G. J., Heterogeneity of human eosinophils. *J. Allergy Clin. Immunol.* 1989, 83, 369–373.
- [10] Pleis, J. R., Lethbridge-Cejku, M., in: *Summary Health Statistics for U.S. Adults: National Health Interview Survey*, Vital Health Stat 2007, 10.
- [11] Matsumoto, K., Appiah-Pippim, J., Schleimer, R. P., Bickel, C. A. *et al.*, CD44 and CD69 represent different types of cell-surface activation markers for human eosinophils. *Am. J. Respir. Cell Mol. Biol.* 1998, 18, 860–866.
- [12] Waschnagg, C., Forsberg, J., Engström, Å., Odreman, F. *et al.*, The human eosinophil proteome. Changes induced by Birch pollen allergy. *J. Proteome Res.* 2009, 8, 2720–2732.
- [13] Yoon, S. W., Kim, T. Y., Sung, M. H., Kim, C. J., Poo, H., Comparative proteomic analysis of peripheral blood eosinophils from healthy donors and atopic dermatitis patients with eosinophilia. *Proteomics* 2005, 5, 1987–1995.
- [14] Ohnmacht, C., Pullner, A., Van Rooijen, N., Voehringer, D., Analysis of eosinophil turnover *in vivo* reveals their active recruitment to and prolonged survival in the peritoneal cavity. *J. Immunol.* 2007, 179, 4766–4774.
- [15] Domachowske, J. B., Dyer, K. D., Adams, A. G., Leto, T. L., Rosenberg, H. F., Eosinophil cationic protein/RNase 3 is another RNase A-family ribonuclease with direct antiviral activity. *Nucleic Acids Res.* 1998, 26, 3358–3363.
- [16] Rosenberg, H. F., Eosinophil-derived neurotoxin/RNase 2; connecting the past, the present and the future. *Curr. Pharm. Biotechnol.* 2008, 9, 135–140.
- [17] Jong, E. C., Henderson, W. R., Klebanoff, S. J., Bactericidal activity of eosinophil peroxidase. *J. Immunol.* 1980, 124, 1378–1382.
- [18] Ackerman, S. J., Liu, L., Kwatia, M. A., Savage, M. P. *et al.*, Charcot-Leyden crystal protein (galectin-10) is not a dual function galectin with lysophospholipase activity but binds a lysophospholipase inhibitor in a novel structural fashion. *J. Biol. Chem.* 2002, 277, 14859–14868.
- [19] Ackerman, S. J., Corrette, S. E., Rosenberg, H. F., Bennett, J. C. *et al.*, Molecular cloning and characterization of human eosinophil Charcot-Leyden crystal protein (lysophospholipase). *J. Immunol.* 1993, 150, 456–468.
- [20] Kubach, J., Lutter, P., Bopp, T., Stoll, S. *et al.*, Human CD4⁺ CD25⁺ regulatory T cells: proteome analysis identifies galectin-10 as a novel marker essential for their energy and suppressive function. *Blood* 2007, 110, 1550–1558.
- [21] Ackerman, S. J., Loegering, D. A., Gleich, G. J., The human eosinophil Charcot-Leyden crystal protein: biochemical characteristics and measurement by radioimmunoassay. *J. Immunol.* 1980, 125, 2118–2126.

- [22] Boehme, S. A., Sullivan, S. K., Crowe, P. D., Santos, M. *et al.*, Activation of mitogen-activated protein kinase regulates eotaxin-induced eosinophil migration. *J. Immunol.* 1999, *163*, 1611–1618.
- [23] Suzuki, M., Kato, M., Hanaka, H., Izumi, T. *et al.*, Actin assembly is a crucial factor for superoxide anion generation from adherent human eosinophils. *J. Allergy Clin. Immunol.* 2003, *112*, 126–133.
- [24] Starosta, V., Pazdrak, K., Boldogh, I., Svider, T., Kurosky, A., Lipoxin A₄ counterregulates GM-CSF signaling in eosinophilic granulocytes. *J. Immunol.* 2008, *181*, 8688–8699.
- [25] Rush, J., Moritz, A., Lee, K. A., Guo, A. *et al.*, Immunoaffinity profiling of tyrosine phosphorylation in cancer cells. *Nat. Biotech.* 2004, *23*, 94–101.
- [26] Zahedi, R. P., Lewandrowski, U., Wiesner, J., Wortelkamp, S. *et al.*, Phosphoproteome of resting human platelets. *J. Proteome Res.* 2008, *7*, 526–534.
- [27] Liu, X., Shu, S., Hong, M.-S. S., Levine, R. L., Korn, E. D., Phosphorylation of actin Tyr-53 inhibits filament nucleation and elongation and stabilizes filaments. *Proc. Natl. Acad. Sci. USA*, 2006, *103*, 13694–13699.
- [28] Wang, S., Zheng, Y., Yu, Y., Xia, L. *et al.*, Phosphorylation of β -actin by protein kinase C-delta in camptothecin analog-induced leukemic cell apoptosis. *Acta Pharmacol. Sinica* 2008, *29*, 135–142.
- [29] Pederson, T., Aebi, U., Actin in the nucleus: what form and what for? *J. Struct. Biol.* 2003, *140*, 3–9.